The United Nations University

GEOTHERMAL TRAINING PROGRAMME
Orkustofnun, Grensásvegur 9,
IS-108 Reykjavík, Iceland

Reports 1995
Number 14

ONE-DIMENSIONAL INTERPRETATION OF SCHLUMBERGER AND TEM RESISTIVITY DATA WITH EXAMPLES FROM TORFAJÖKULL, S-ICELAND

Fred M. Tugume
Geological Survey and Mines Department,
Ministry of Natural Resources,
P.O. Box 9, Entebbe,
UGANDA

ABSTRACT

In this report, a brief discussion covering the basic principles, field techniques, instrumentation and interpretation of Schlumberger and TEM soundings is given. As an example, Torfajökull geothermal field in S-Iceland was chosen. 33 TEM soundings from the field were interpreted using a one-dimensional inversion programme. The quality of the Schlumberger data (13 soundings) was found to be low. From the results of the TEM soundings, seven resistivity profiles and four iso-resistivity maps were made. The results show a well defined resistivity anomaly. Based on experience from other high-temperature geothermal fields in Iceland, the resistivity structure is interpreted in terms of geothermal activity. The inferred geothermal activity can be correlated with a caldera found in the survey area.

1. INTRODUCTION

In Uganda, limited studies of the country's geothermal resources have been carried out. A geothermal exploration project (UGA/92/002 & UGA/92/E01), which was initiated after the visit of the technical adviser for United Nations Department for Development Support and Management Services to Uganda, included surface geological exploration and analyses of the chemical properties of water samples got from the geothermal fields. No geophysical methods have been applied yet as there has been no geophysicist among the already established geothermal group under Geological Survey and Mines Department of the Ministry of Natural Resources. As a result, a geophysicist was recruited and immediately sent to attend the UNU G.T.P. in Iceland.

The six months course attended by the author, included introductory lectures, covering geothermal exploration, production and utilisation for the first five weeks. The rest of the programme included specialized training, field work and trips.

As a part of the specialised training, the author was introduced to the gravity and magnetic methods but most emphasis was on resistivity methods especially Schlumberger and Transient Electromagnetic (TEM) soundings. This report discusses the role of resistivity methods in geothermal exploration. The

Schlumberger and TEM sounding methods are discussed, both theoretical and practical aspects. As a part of the training, the author took part in data collection at Krísuvík SW-Iceland where Schlumberger and TEM methods were applied. Emphasis was laid on the problems faced in the field and where precautions should be taken. TEM data collected from 33 stations in Torfajökull geothermal field are interpreted using the one-dimensional inversion software, written and installed on PC by the staff at Orkustofnun. Also Schlumberger data collected from 13 stations were interpreted using one-dimensional inversion software also written and installed by Orkustofnun staff.

Interpretation of the data from Torfajokull gave the author the experience of relating the resistivity structure to the geothermal activity and the geology of the area. Results of interpretation are discussed and presented in the form of resistivity sections and iso-resistivity maps.

2. ROLE OF RESISTIVITY METHODS IN GEOTHERMAL EXPLORATION

2.1 Geothermal exploration methods

Geothermal exploration is a multi disciplinary task using several methods. They can be divided into the following categories, geological, geochemical, geophysical methods, and exploratory drilling. Each of the mentioned methods plays different parts at different stages. Geological and geochemical exploration are often applied as the first stages of the exploration. They are often used to select feasible prospects, for further exploration by the normally more expensive geophysical methods and exploratory drilling.

Geological exploration
Geological exploration is normally the first stage in geothermal exploration. It should preferably comprise of the following: Mapping of surface manifestation and geothermal alteration, volcanic history, that is, age of volcanics and stages in evolution, detailed mapping of dip and strike of geological units and orientation of intrusives and faults, structural analyses of faults and dykes, cross-section showing the stratigraphic units and variations in thickness along and perpendicular to strike, and collection of rock samples from all units for later petrological comparison with boreholes.

Geochemical exploration
In geothermal exploration geochemical methods play the following parts. Assessment of reservoir temperature and water and steam quality, location of recharge areas and evaluation of direction of subsurface fluid flow, and evaluation of mixing of hot and cold water upflow in geothermal systems and of possible boiling processes.

Geophysical exploration
Surface geophysical methods are very important in geothermal exploration. They can be divided into structural methods which give information on geological structures and methods that are sensitive to anomalies directly connected to the geothermal activity. The gravity and magnetic methods are examples of structural methods, while resistivity methods map resistivity anomalies which are, in most cases, directly associated with the geothermal resources.

In geophysical exploration, data are usually presented in two ways, as iso-value maps and as cross-sections. They are summaries of the observations and are not geological nor geothermal interpretations. Qualitative conclusions, such as location, size and shape of anomalous body, strike of faults or dykes, can be drawn from the maps and cross-sections.

Resistivity methods have been found to be the most powerful methods for geothermal exploration

(Árnason and Flóvenz, 1992; Eysteinsson et al., 1993). The reason for this is that the resistivity of rocks is strongly affected by the geothermal activity. This makes the resistivity generally the most diagnostic physical parameter for geothermal activity that can be measured by surface exploration.

Resistivity surveying has sometimes led to identification of previously unknown geothermal systems, even where no surface manifestations are found. They can sometimes be used to locate aquifers and to estimate porosity and physical conditions within a geothermal system.

Exploratory drilling
Exploratory drilling is normally much more expensive than the surface exploration. It is therefore usually not applied until at late stages of the exploration and at promising targets. The purpose of this is to prove the existence of a geothermal reservoir, find the base temperature and investigate the chemical composition of the fluid. Further, the first estimate of the reservoir parameters are found.

2.2 Different resistivity methods

The common principle of all surface resistivity methods is to measure signals at the surface from the introduced currents in the earth (Hersir and Björnsson, 1991). By relating the measured signals to the source strength, information is obtained about the subsurface resistivity structure. Resistivity methods are normally divided into two categories according to the source signal, that is, into controlled source and natural source methods. It is also customary to classify resistivity methods according to the time dependence of the source signal. Direct current (DC) methods use time independent sources while the electromagnetic methods use time varying sources and rely on electromagnetic induction in the earth.

Direct current methods
In DC methods a time independent current distribution is set up in the subsurface by transmitting constant current into the earth, normally from the surface. By measuring associated potential difference at the surface, information is obtained about the resistivity structure.

DC methods are also subdivided into various sub-categories, such as Schlumberger sounding, Head-on profiling, Dipole-dipole profiling and sounding, depending on the type of electrode arrangement applied. Soundings refer to measurements of resistivity as function of depth using different distances between current electrodes. Profiling measures the lateral changes in resistivity at nearly constant depth by measurements taken with fixed distances between current electrodes made at different points on the surface.

Electromagnetic methods
Electromagnetic resistivity methods make use of an alternating current induced in the earth. It may be artificially induced or be a natural signal. Electromagnetic methods are divided into subcategories also. Natural source methods include magnetotellurics and audio-magnetotellurics. Controlled source electromagnetic methods include the, by now widely used, Transient electro magnetic (TEM) methods.

In the TEM sounding method the current in the ground is generated by a man made time varying magnetic field. The current distribution and the decay rate of the secondary magnetic field depends on the resistivity structure of the earth and can be interpreted in terms of subsurface resistivity structure.

The MT method uses time variations in the earth´s magnetic field as a source for induced currents in the earth. It has been used to investigate deep structures of the crust and the upper mantle and has been successful in mapping bodies with anomalous low-resistivity. Good correlation has been found in many areas between anomalous high heat flow and depth to a low-resistivity bodies observed by MT (Kaufman and Keller, 1981).

2.3 Connection between resistivity and geothermal activity

Resistivity of water saturated rocks is dependent on porosity, the resistivity of the water, temperature, and alteration minerals. These factors often interact in a complicated way. Equations have been proposed to describe the influence of the different factors. These equations are based on the measurements of resistivity in different rock samples under different conditions.

If electrical conduction is mainly in the saturating fluid, Archie's law (Archie, 1942) describes how resistivity depends on porosity and the resistivity of the fluid:

$$\rho = \rho_w a \Phi_t^{-m} \tag{1}$$

where

ρ = Bulk resistivity (Ωm);
ρ_w = Resistivity of the pore fluid (Ωm);
ϕ_t = Porosity;
a = Empirical parameter, usually around one;
m = Cementation factor, usually around 2.

The following relation (Dakhnov, 1962) describes how resistivity of the pore fluid decreases with increasing temperature, due to the increasing mobility of ions, through the relation:

$$\rho_w = \frac{\rho_{w_o}}{1+\alpha(T-T_o)} \tag{2}$$

where

ρ_{wo} = Resistivity of the fluid at temperature T_o (Ωm);
α = Temperature coefficient, α=0.023°C^{-1} for T_0=23°C and 0.025 °C^{-1} for T_o=0°C.

The resistivity of the pore fluid is nearly inversely proportional to the concentration of dissolved ions. For NaCl solutions at $T\leq$ 0°C the dependence on concentration, C, is given as (Keller and Frischknecht, 1966):

$$\rho = 9.545 C^{-0.937} \cong \frac{10}{C} \tag{3}$$

Combining Equations 1 and 2 gives an expression that can be used for relating temperature and resistivity. This has helped in making iso-temperature maps in the Reykjanes peninsula SW-Iceland (Georgsson, 1984).

The bulk resistivity is decreased by interface conduction along contact surfaces between rock and water. Experiments show that interface conduction depends on the magnitude of the internal surface (porosity) and its nature (surface conditions). The reasons for interface conductivity is the presence of ionic double layer at the rock-water interface. Conduction can also take place in conducting minerals in the rocks. Geothermal alteration of rocks often produces conductive minerals, such as clays and zeolites. Conduction in rocks can be viewed (Flóvenz et al., 1985; Stefánsson et al., 1982) as a conduction in parallel resistors where the current mainly passes through the o ne with lower resistance. Experiments

show that Archie's law is only valid for conductive solutions $\rho_w \leq 2\ \Omega m$. The type of alteration minerals formed depends upon the temperature, chemical composition of fresh rocks, and saturating fluid (Kristmannsdóttir, 1979). The observed resistivity structure of low salinity geothermal systems in Iceland, where basaltic rocks are abundant, indicates correlation between temperature, alteration and resistivity (Árnason, 1993). Below low-resistivity layer coinciding with clay alteration minerals, it is common to have high-resistivity at the centre of the high-temperature field. It is believed that the change in alteration minerals from the conductive clay minerals to the more resistive chlorite and epidote is the reason for high-resistivity below low-resistivity.

3. THE SCHLUMBERGER SOUNDING METHOD

3.1 Theoretical basis

This section discusses the theoretical basis of the Schlumberger soundings at the surface of a layered earth (see for example Koefoed, 1979).

In the Schlumberger array, two potential and two current injection electrodes are placed along a straight line. The array is symmetrical around the midpoint O. The setup is shown in Figure 1, where the current electrodes are placed at A and B and the potential electrodes are placed at M and N. The distances are given as, OA = OB = S and MO = ON = P. The depth of exploration is increased by increasing the distance S from the centre. The distance between the potential and the current electrodes are $2P$ and $2S$, respectively, where P is much smaller than S. Current is transmitted to the ground through electrode A and extracted through B.

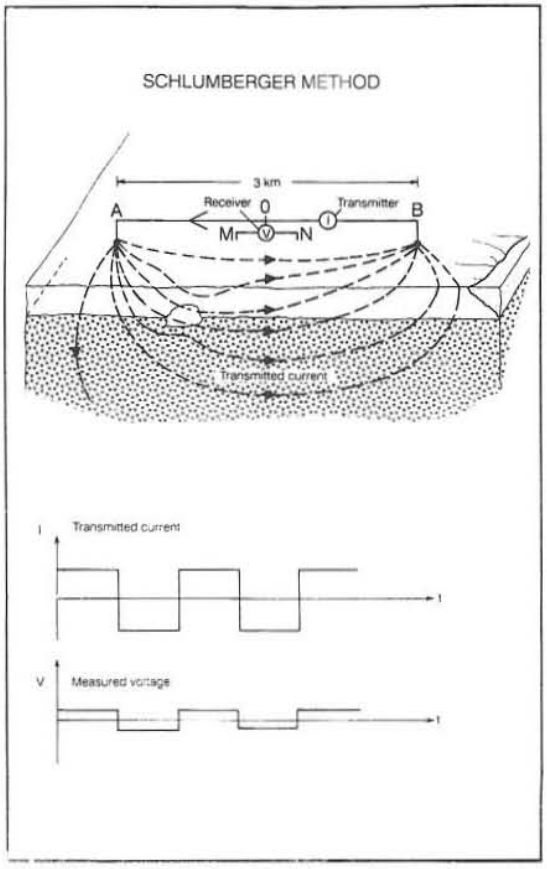

FIGURE 1: The Schlumberger arrangement

In the case of the homogeneous earth, the potential at a distance r from the current source injecting current I is given as

$$V(r) = \frac{\rho I}{2\pi r} \tag{4}$$

At position A, current I is injected and at position B, the same amount of current is extracted. The potential V_N at position N, is the sum of the potentials from A and B. Thus

$$V_N = V_N(A) + V_N(B) = \frac{\rho(+I)}{2\pi(S+P)} + \frac{\rho(-I)}{2\pi(S-P)} \tag{5}$$

which implies that

$$V_N = \frac{\rho I}{2\pi}\left[\frac{1}{S+P} - \frac{1}{S-P}\right] \tag{6}$$

In a similar manner it is seen that the potential at M is

$$V_M = \frac{\rho I}{2\pi}\left[\frac{1}{S-P} - \frac{1}{S+P}\right] \tag{7}$$

The potential difference between M and N is ΔV, and is given as

$$\Delta V = V_M - V_N = 2\frac{\rho I}{2\pi}\left[\frac{1}{S-P} - \frac{1}{S+P}\right] = \frac{2\rho IP}{\pi(S^2 - P^2)} \tag{8}$$

Solving for ρ, this becomes

$$\rho = \frac{\Delta V}{2IP}\pi(S^2 - P^2) \tag{9}$$

If the earth is not homogenous, the resistivity calculated from the measured values of current and potential is taken as the apparent resistivity ρ_a, defined as in the equation below,

$$\rho_a = \frac{\Delta V}{I}K \tag{10}$$

where K is the geometric constant, given as

$$K = \frac{\pi(S^2 - P^2)}{2P} \tag{11}$$

To relate the measured apparent resistivity to the actual resistivity structure of the layered earth, we need to express the voltage in terms of the relevant resistivity parameters. We consider the case of layered half space with N layers. Each layer is assumed homogeneous and isotropic with resistivity ρ_i and thickness d_i (the Nth layer is infinitely thick). The potential in the ith layer, due to a current source at r=0, z= 0 on the surface, is in cylindrical coordinates, given as

$$V_i(r,z) = \frac{\rho_1 I}{2\pi}\int_0^\infty (C_i(\lambda)\cosh[\lambda(z-h_i)] + D_i(\lambda)\sinh[\lambda(z-h_i)])J_o(\lambda r)\,d\lambda \tag{12}$$

where

C_i & D_i = Functions of λ;
λ = Variable of integration;

J_o = Bessel function of order zero;
ρ_1 = Resistivity of the first layer;
h_i = Depth of the top of the ith layer;
r = Radial distance from the source current;
z = Depth below surface.

The potential has to obey the following boundary conditions:

1. $V_i \rightarrow 0$ as $r \rightarrow 0$, for $i = 1, 2, 3, \ldots\ldots, N$;
2. $V_N \rightarrow 0$ as $z \rightarrow \infty$;
3. $V_i = V_{i+1}$ at $z = h_{i+1}$;
4. $J_{iz} = J_{i+1z}$ at $z = h_{i+1}$.

Condition 4 implies that when $z=h_{i+1}$

$$\frac{1}{\rho_i}\frac{\partial V_i}{\partial z} = \frac{1}{\rho_{i+1}}\frac{\partial V_{i+1}}{\partial z} \tag{13}$$

which in turn implies the following condition at the surface:

5. $\partial V_1/\partial z = 0$ for $r \neq 0$ and $z=0$.

These conditions can be used to determine the coefficients D_i and C_i. For the *Nth* layer the second boundary conditions implies that $D_N=-C_N$. Defining the function $K_i = -C_i/D_i$, we have $K_N = 1$, and conditions 3 and 4 can be shown to imply that K_i is given by the recurrence relation

$$K_i = \frac{K_{i+1} + \rho_i/\rho_{i+1}\tanh(\lambda d_i)}{\rho_i/\rho_{i+1} + K_i\tanh(\lambda d_i)} \tag{14}$$

where ρ_i and d are the resistivity and thickness of the ith layer. It can furthermore be shown, by condition 5, that $D_1 = -1$ and therefore

$$V_1(r,z) = \frac{\rho_1 I}{2\pi}\int_0^\infty [K_1\cosh(\lambda z) - \sinh(\lambda z)]J_o(\lambda r)\,d\lambda \tag{15}$$

At the surface, $z=0$, Equation 15 becomes

$$V_1(r) = \frac{\rho_1 I}{2\pi}\int_0^\infty K_1 J_0(\lambda r)\,d\lambda \tag{16}$$

This equation, along with the recurrence relation (Equation 14), gives the potential at the distance r from a point current source injecting the current I at the surface of a layered half space. Equation 16 can now be used to calculate the potentials V_N and V_M in the Schlumberger array and hence the apparent resistivity for a given layered earth.

The depth of penetration of Schlumberger soundings, is not only a function of the distance between the current electrodes, *2S*. It is in fact controlled by the shortest distance between a current electrode and a potential electrode, *S-P* (Árnason, 1984). For the same *S* and different *P*, different values ρ_a reflect resistivity at different depth. For instance, if the difference *S-P*, in a two layer case, is much less than the depth to the boundary, the measured ρ_a value will be dominated by the resistivity value of the first layer, ρ_1, independent of the distance between the current electrodes. When *S-P* becomes much larger than the depth to the layer boundary, the current will penetrate the second layer and the apparent resistivity will approach the resistivity of the second layer.

3.2 Instrumentation

The conventional instruments used in Schlumberger soundings consist of potential difference receiver with data logger, current transmitter, power source, electrodes and electric cables usually on reels. For communication walkie-talkies are necessary.

The potential is measured with the receiver between two potential electrodes. Non-polarizing electrodes made of copper rod immersed in a porous vessel filled with a saturated solution of copper sulphate are recommended, not metallic electrodes. The receiver may be an IP receiver or one digitally computerized with microprocessor like the one used in Iceland.

The current transmitter drives current through the current electrodes to the ground. The energy source is usually car batteries or current generator depending on the demand. Current electrodes can be made of iron bars or spiral blades. Iron bars should be maximum 50 cm long. Electric wires which connect the electrodes to the transmitter should always be wound on reels for easy use in field and storage. The reels should be made of light material.

It is important to choose instruments with the correct specifications in order to suit the workload of the given task. The instruments should be checked in the pre-field work preparations to see that they fit the required conditions. For instance the cables should be checked for current leakage before and after the field work. If an A.C. generator is used as a power source, it should be in good mechanical conditions and have enough fuel. In the case of batteries make sure that they are rechargeable and a battery charger available. Potential difference receiver should be checked by qualified personnel. It is always advisable to follow the user´s guide when collecting data, to avoid unnecessary errors.

3.3 Field procedure

In a reconnaissance survey, suitable sampling sites should be chosen most preferably along the straight lines, but often this is not possible due to topography and vegetation of the area. The distance between the sites should be about 1-2 km but the intensity might be increased inside an area of particular interest.

After deciding on the site and the direction of the sounding with the help of a compass, measurements can start. The transmitter, the power source and the receiver are located at the centre of the profile and wires laid out in opposite directions from the centre. The transmitter is connected to the power source, and the current carrying cables connected to the output of the transmitter. Cables connect the potential electrodes to the receiver.

In Iceland, three to four people carry out the sounding but in other countries where conditions (topographic and vegetational) are different, more than ten people may be needed. Two people move the current electrodes outwards while, one or two remain at the centre where he/she record and plot the

apparent resistivity.

The distance between the current electrodes AB is considerably larger than that of the potential electrodes MN and the minimum is always AB>4MN. The current electrode spacing is increased in steps and the apparent resistivity measured for AB values equally distributed on log-scale. The distances at which readings are taken are marked on the cable and colour coding of the distances is recommended. Such coding helps preventing readings to be taken with a current electrode at a wrong place. The maximum MN/2 used in Iceland is 100 m and the maximum AB/2 is usually 2000 m.

With increased distance between the current electrodes, the current penetrates deeper. When AB/2 is large (AB/2≥1000), the received signal is usually weak. In this case the signal can be enhanced by improving the current electrode contact by putting more than two poles and taking several repeated measurements. Despite these measures, the potential signal eventually drops below the noise threshold. In order to increase the potential signal the potential electrode spacing is increased but should be kept such that AB>4MN.

The apparent resistivity is plotted as a function of AB/2 on a log-log paper and is then ready for interpretation.

4. THE TEM SOUNDING METHOD

4.1 Theoretical basis

TEM methods measure the earth's resistivity by use of controlled source electromagnetic transients. In the central loop TEM method, a magnetic field of a known strength is built up by transmitting a constant current into a source loop (Figure 2). The current is then turned off abruptly. The decaying magnetic field induces currents in the earth and hence a secondary magnetic field decaying with time. The decay rate of this secondary field is monitored by measuring the induced voltage in the receiver coil at the centre of the transmitter loop. The current distribution and the decay rate of the secondary magnetic field depend on the resistivity structure of the earth.

In transient soundings the transient response voltage in the receiver coil at the centre of the circular transmitting loop of radial r is given as a function of t as (Árnason, 1989)

$$V(r,t) = A_r n_r A_s n_s \frac{I\mu_0}{\pi^2 r^3} \int_0^\infty Re[E^e(r,\omega)]\cos(\omega t)\, d\omega \qquad (17)$$

where

t = Time passed since the current in the transmitter loop was turned off;
A_r = Cross-sectional area of the receiver coil m^2);
n_r = Number of windings in the receiver coil;
μ_o = Permeability of free space (mkg/C^2);
A_s = Cross-sectional area of the current loop (m^2);
n_s = Number of windings in the current loop;
$V(r, t)$ = Transient voltage (V);
$E^e(\omega,r)$ = Earth response factor

The earth response factor $E^e(\omega,r)$ is given as

$$E^e(\omega,r) = 2r^2 \int_0^\infty \lambda \frac{S_0}{S_0 - T_0} J_1(\lambda r)\, dr \qquad (18)$$

where S_o, T_o contain the parameters of the layered earth. They are determined by the recurrence relations similar to those described in Chapter 3.

For a homogenous half space with conductivity σ the induced transient voltage in the receiver is, for late times, proportional to $\sigma^{3/2}$ and $t^{-5/2}$. It is customary to express the transient response as the late apparent resistivity rather than the induced voltage:

$$\rho_a(r,t) = \frac{\mu_o}{4\pi}\left[\frac{2\mu_o A_r A_s n_s I}{5 t^{5/2} V(r,t)}\right]^{2/3} \qquad (19)$$

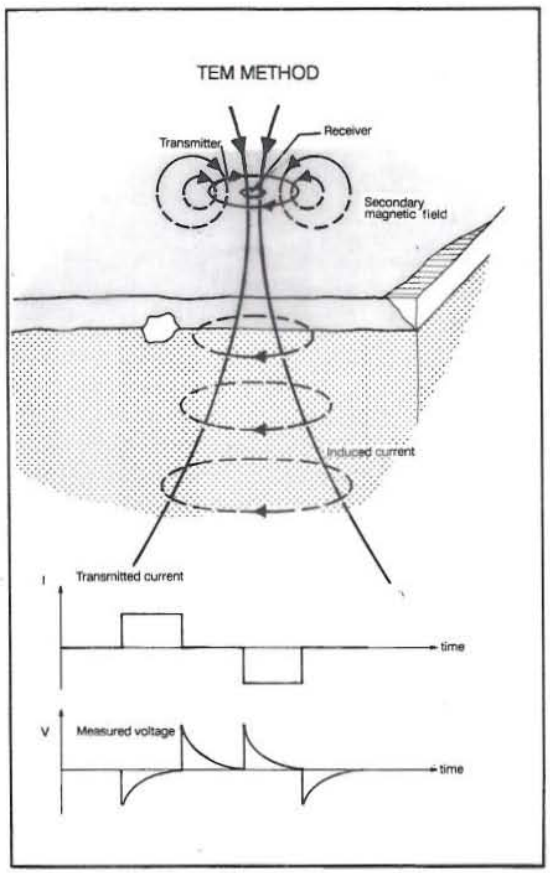

FIGURE 2: TEM sounding configuration

In case of homogeneous earth, this apparent resistivity approaches the true resistivity of the earth for late times.

4.2 Instrumentation

The TEM instruments used in Iceland are Protem/EM 37 from Geonics Ltd. They consist of a current transmitter, a transmitter loop, a generator, a receiver with built in data logger, a receiver coil with an effective area of 100 m^2, and a receiver loop with an effective area of 8125m^2 can be used.

The receiver monitors the decay rate of the secondary (transient) magnetic field by measuring the induced voltage in the receiver coil located at the centre of the transmitter loop (Figure 2). Both the transmitter and receiver timings are controlled by synchronised high precession crystal clocks. The current transmitted in the source loop is in a box wave form with each cycle divided into four time intervals of equal length (a positive current on, current off, negative current on, and current off). The induced voltage is measured by the receiver each time the transmitted current is turned off.

The equipment can be run at different frequencies. It is usually run at two different frequencies (high and low). On high frequency the repetition rate of the transmitted current signal is 25 hz, with current on and current off segments of 10 ms. On the low frequency the repetition rate is 2.5 hz, with the current on and current off intervals of 100 ms. After the current turn off, the decay signal is measured at 20 time gates, or channels, logarithmically distributed in time. On the high frequency the receiver measures the

1st channel (time gate) at 0.087 ms and the 20th channel at 7.040 ms after the current is turned off. On the low frequency, the channels are shifted by a factor of 10 with respect to the high frequency so that the first and last channels measured are 0.87 ms and 70.40 ms after the turn off respectively. By measuring on the two frequencies, the decay rate of the secondary magnetic field is monitored at 30 time gates distributed logarithmically in time, with 10 points per decade, over the interval at 0.087 to 70.40 ms after the turn off and with 10 points overlapping.

4.3 Field procedure

In Iceland the current cables are usually laid in a 300 by 300 m^2 square loop but in some cases a 200 by 200 m^2 is thought to be sufficient. The current transmitted is usually in the range of 20-30 A. In order to suppress both external and internal noise in the data, the measured transient voltage is stacked over many cycles. Furthermore, since the transient voltage decreases rapidly with time, the low frequency part is usually measured both with the receiver coil and a flexible loop of relatively large area compared to the receiver coil, to give a higher output signal. Usually the high frequency signals are measured in 5 to 8 data sets where each set is stacked over 256 cycles. On the low frequency there are measured about 4 data sets stacked over 512 cycles with the standard receiver coil and 5 to 8 sets stacked over 512 cycles with the flexible receiver loop.

Each data set is automatically stored in the memory of the data logger with information on the transmitter loop area, transmitted current, frequency, gain settings, and other book keeping information. The collected data is transferred from the data logger to the a personal computer for data processing and inversion.

5. ONE-DIMENSIONAL INVERSION OF RESISTIVITY DATA

The preceding chapters described briefly how the apparent resistivity curves for Schlumberger and TEM soundings can be calculated for given layered earth models. This is a solution to what is called the forward problem i.e. to determine the response that would be measured if the earth had a given layered structure. Interpretation of measured resistivity data in terms of layered earth models can now in principle be done by forward modelling. Forward modelling consist of guessing a layered structure and comparing the calculated response of the model to the measured data. By visual inspection of the difference between the measured and calculated response a new model is guessed. This is continued until satisfactory agreement is obtained and the resulting model is taken as the interpretation of the measured curve. Such a procedure has been used and is in some cases still applied, for example in two-dimensional modelling, but it is often rather time consuming.

One-dimensional interpretation is nowadays usually done by inversion programmes. An inversion programme contains a forward algorithm and an inversion algorithm (Árnason, 1989). The inversion algorithm is a procedure that calculates, from the difference between calculated response of a given model and measured data, adjustment to the model parameters such that better agreement is obtained. This is normally done by calculating how a slight change in each of the model parameters effects the response. This can be used to determine changes in the parameters which result in better agreement with the measured response. An inversion programme applies a forward and an inversion algorithms iteratively until the difference in the calculated and measured responses cannot be further reduced. Several inversion algorithms have been developed. Among the most commonly used algorithms is the so called Levenberg-Marquardt non-linear least-squares algorithm (a detailed description of this algorithm is outside the scope of the present work but can be found in Árnason, 1989). This algorithm is robust and rarely fails to converge.

5.1 Schlumberger data

A one-dimensional inversion algorithm for Schlumberger soundings, according to the above described procedure, has been implemented in the computer programme SLINV. The programme was written and installed on PC computers by the Orkustofnun staff (Árnason and Hersir, 1988).

The programme works in such a way that it reads the measured data points (apparent resistivity as a function of AB/2) and prompts for a starting model. The interpreter guesses, by visual inspection of the data curve, the number of layers and the initial model parameters, that is the resistivity values and thickness of the layers. Each model parameter can be a free or fixed parameter.

The programme iteratively adjusts the values of the free model parameters to get the best fit between the measured curve and the calculated curve from the model. The programme does not change the number of layers during the iteration process. This implies that it is necessary to try models with different number of layers to find the model that best fits the data.

The programme calculates the apparent resistivity values from the given one-dimensional model using the gradient approximation. This means, it is assumed that the receiving dipole (the distance between potential electrodes) is infinitesimally short compared to the transmitter dipole. This implies that the actual electrode configuration in the sounding is not simulated and only one apparent resistivity value can be assigned to each value of AB/2.

From Equations 9 and 16, it is easily seen that, in the gradient approximation ($P<<S$), the apparent resistivity is given as a function of r=AB/2 by the formula

$$\rho_a(r) = r^2 \int_0^\infty K_1(\lambda) J_1(\lambda r) \lambda \, \partial\lambda \qquad (20)$$

The kernel function $K_1(\lambda)$ contains the model parameters and is given by the recurrence relation (Equation 14). Figure 3 shows an example of a Schlumberger sounding inverted by the programme SLINV.

5.2 TEM data

The general inversion approach, as described at the beginning of this section, has also been implemented in a one-dimensional inversion programme TINV for TEM soundings. This programme was written and installed by the Orkustofnun staff (Árnason, 1989).

The programme assumes that the field data is collected with equipment where the current transmitted in the loop is turned off linearly from maximum to zero and that the time values, at which the apparent resistivity values are given, are equally spaced in logarithm of time after the current has become zero. The programme assumes that data is collected with a circular loop. If this is not the case the actual transmitter loop is simulated by a circular loop having the same area.

The programme works in such a way that it reads the measured data points (apparent resistivity as a function of time) and prompts for a starting model. The interpreter guesses, by visual inspection of the data curve, the number of layers and initial model parameters, that is the resistivity values and thickness of layers. The programme iteratively adjusts the free model parameter to get the best fit between the measured curve and the calculated curve from the model. Figure 4 shows an example of one-dimensional inversions of a TEM-sounding using the programme TINV.

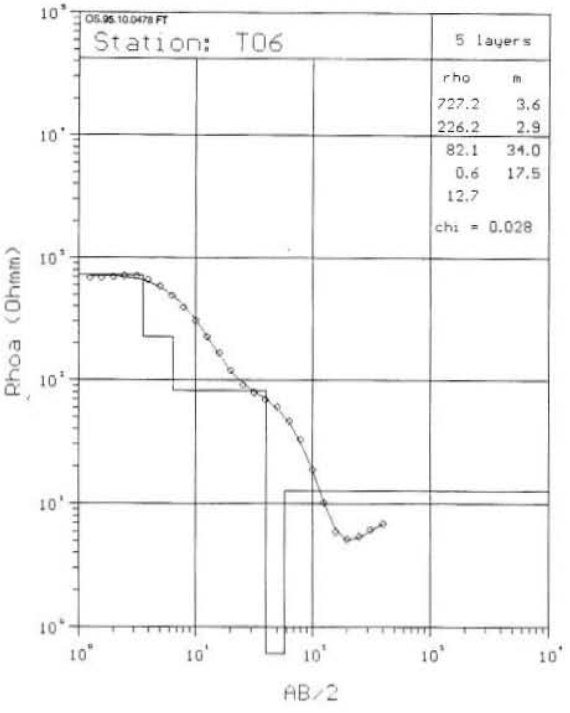

FIGURE 3: One-dimensional interpretation of Schlumberger sounding T06 from Torfajökull, circles show data, solid line refers to the model

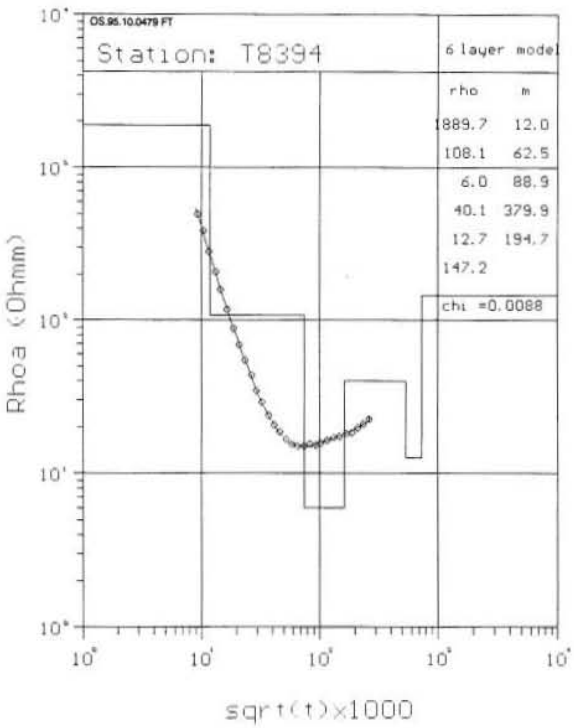

FIGURE 4: One-dimensional interpretation of TEM sounding T8394 from Torfajökull, circles show data, solid line refers to the model

6. THE TORFAJÖKULL GEOTHERMAL FIELD

Results of a resistivity survey in Torfajökull, central south Iceland, are presented here and taken as an example of the use of one-dimensional inversion of resistivity data. This survey was carried out by the Orkustofnun staff. Schlumberger data was collected in 1972-1975 and TEM data in 1993-1995. The data presented in this report are only part of the whole data set covering the southwestern part of the large geothermal area around Torfajökull.

6.1 Geological settings

The geology of the Torfajökull area has been described by Ívarsson (1992). The Torfajökull volcano is located on the northern edge of the southern volcanic flank zone. Immediately to the northeast is the Veidivötn fissure swarm which is a normal spreading ridge segment within the eastern rift zone, characterized by tholetic volcanics. To the west and south are central volcanoes and fissure swarms belonging to the southern flank zone.

The Torfajökull massif is elongated in NW-SE direction, perpendicular to the strike of the eastern rift zone and has approximate dimensions of 20x30 km^2. It rises from a 600 m platform to 1200 m. Its southern and eastern parts are eroded with broad outwash-floored valleys and deep gullies. The northern part is more level with conical hills, block lava flows and shallow stream beds.

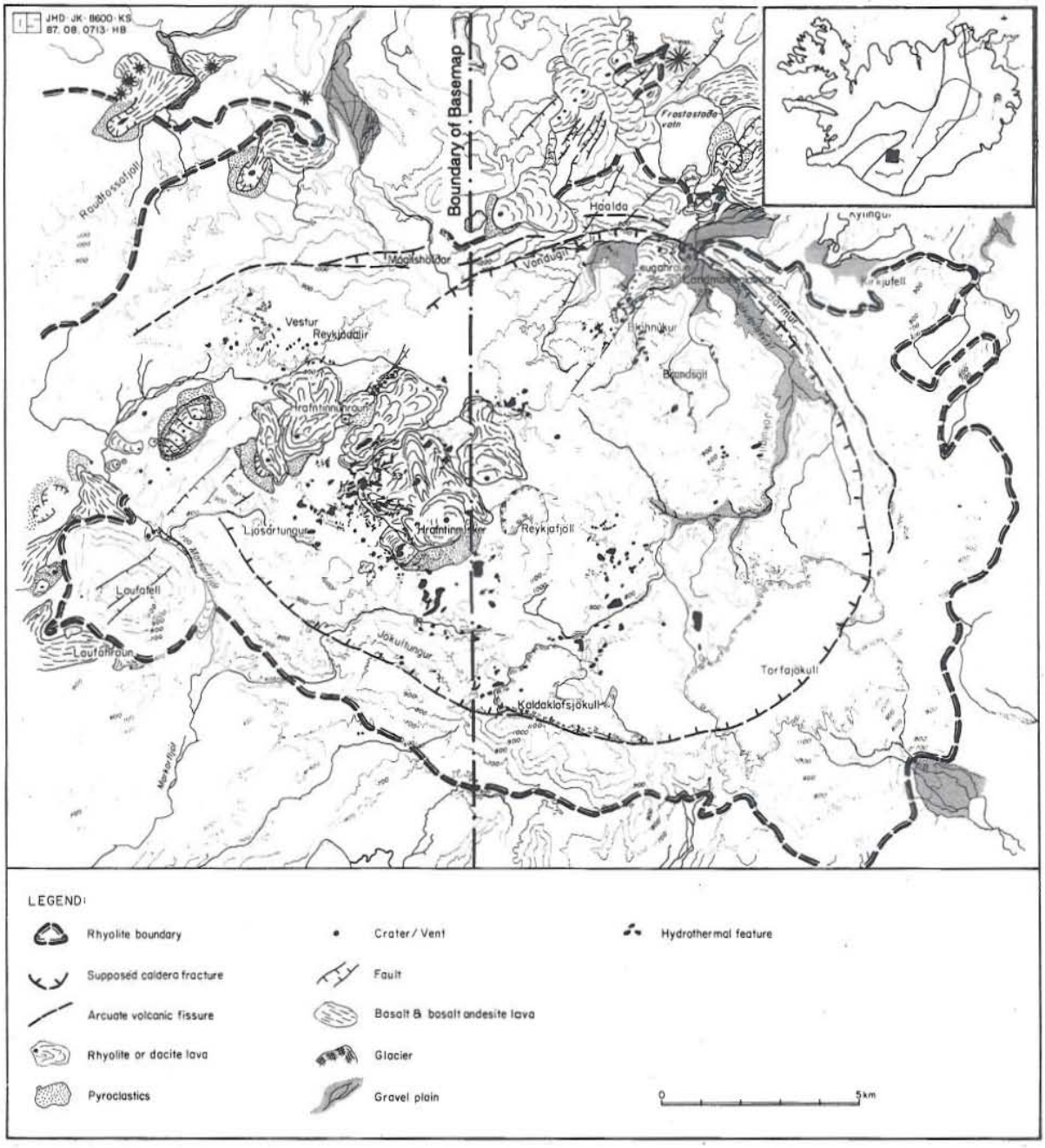

FIGURE 5: Simplified geological map of the Torfajökull area (from Arnórsson et al., 1987)

The drainage pattern is not radial. Half of the area is drained by a single river system flowing through a gap in a ring structure which is thought to reflect buried caldera and the drainage pattern appears partly to follow the trend established by the ring structure. This suggests that drainage is guided by a zone of weakness inside the ring structure indicating perhaps dooming of the ring and subsequent erosion along faults on the perimeter of the dome.

The total area which Torfajökull volcano covers is nearly 500 km^2, of which 280 km^2 are rhyolites, and the rest are intermediate hyaloclastic ridges and pillow lava and postglacial rocks. The abundance of acidic rocks makes Torfajökull volcanic system somewhat distinct from other volcanic systems in Iceland, where basaltic rocks are generally dominant. Figure 5 shows a simplified geological map of Torfajökull area.

6.2 Geothermal surface manifestations

Geothermal manifestations are abundant in the Torfajökull area. They are mainly found in the western part of the ring structure (caldera) and in the southern and south eastern part (Figure 5).The manifestations consist mostly of steaming ground which is, as a rule, intensely altered by acid leaching. Steam heated waters of the bicarbonate and acid sulphate types are relatively common. In the northeastern part of the field, sodium chloride waters occur. They represent boiled and variably mixed reservoir water. This water is higher in chloride than geothermal water associated with basaltic rocks in Iceland. The reason is considered to be higher chloride content of rhyolites as compared with basaltic rocks.

Fumarole steam at Torfajökull generally contains 0.2-0.4% total gas by volume. CO_2 is always the dominant gas content (>70%) but H_2S and H_2 amount to 2-8 and 0-10% respectively. Helium isotope ratios as high as 23.4 times atmospheric have been observed in fumarole steam. These high ratios are taken to indicate a relatively primitive undegassed mantle source (Arnórsson et al., 1987; Ívarsson, 1992).

The natural heat output has been estimated to be equal to 190-930 kg/s of steam. The stored heat in the uppermost 3 km of the reservoir was estimated by Pálmason (1980) as 281×10^{18} J.

7. INTERPRETATION OF THE TORFAJÖKULL RESISTIVITY DATA

7.1 Interpretation and location of the soundings

The data collected in this area were interpreted using one-dimensional interpretation. The TEM data are of good quality. The Schlumberger data are on the other hand from the early years of the application of resistivity methods in Iceland and turned out to be of low quality. After processing and interpretation of the Schlumberger data, it was not found to add any information to the TEM data. The TEM data were interpreted using the TINV programme (details of the programme are discussed in Chapter 5). The final model is obtained when the average difference between measured and calculated values becomes less than 1%. The sounding curves and their interpretation are shown in Appendix I. Location of the TEM soundings is shown in Figure 6. Table 1 shows the comparison of a Schlumberger sounding (Figure 3) and a TEM sounding (Figure 4) carried out in almost the same location.

TABLE 1: Comparison of results of a TEM and Schlumberger sounding in almost the same location

Schlumberger sounding T06		**TEM sounding T8394**	
Resistivity (Ωm)	**Depth (m)**	**Resistivity (Ωm)**	**Depth (m)**
727.2	3.6	1889.7	12
226	2.9	108.1	62.5
82.1	34	6	88.9
0.6	17.5	40.1	379.9
12.7		12.7	194.7
		147.7	

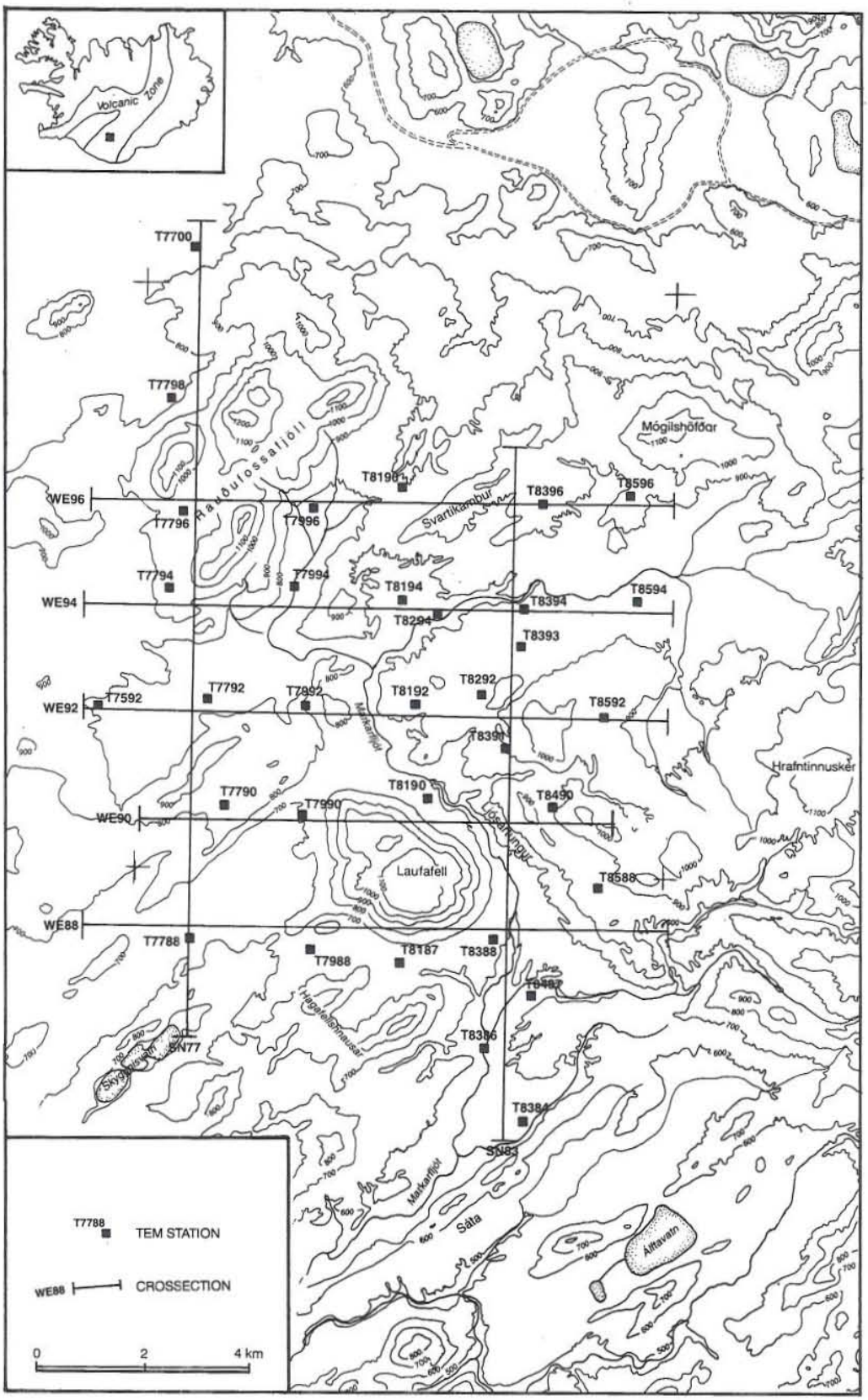

FIGURE 6: Location of TEM soundings and cross-sections in the Torfajökull area

The layered resistivity models obtained from the TEM-soundings were used to compile resistivity cross-sections and iso-resistivity maps at different elevations. The locations of the cross-sections are shown in Figure 6.

7.2 The resistivity cross-sections and iso-resistivity maps

The data presented here lies between 7085 to 7101 northwards and 0575 to 0585 eastward on the UTM coordinates. Based on the TEM data obtained from 33 stations, seven cross-sections were made in this area, 2 running from south to north and the rest running from west to east. Four iso-resistivity maps were also drawn, at altitudes of 700, 500, 300, and 100 m a.s.l.

Resistivity cross-section SN 77 (Figure 7)
The cross-section runs from south to north on the western part of the surveyed area with seven soundings projected on it. A high-resistivity layer of 100 to 6000 Ωm was detected at the top. The biggest and smallest thickness of the top layer was detected in soundings T7794 and T7798, respectively. The section shows 50-100 Ωm resistivity layers at two different depths in the central part of the cross-section. At the extreme ends of it values between 25-50 Ωm were detected and these seem not to be connected. Resistivity values lower than 25 Ωm were recorded on all stations except on T7790 and T7700. All the soundings show decreasing resistivity with depth.

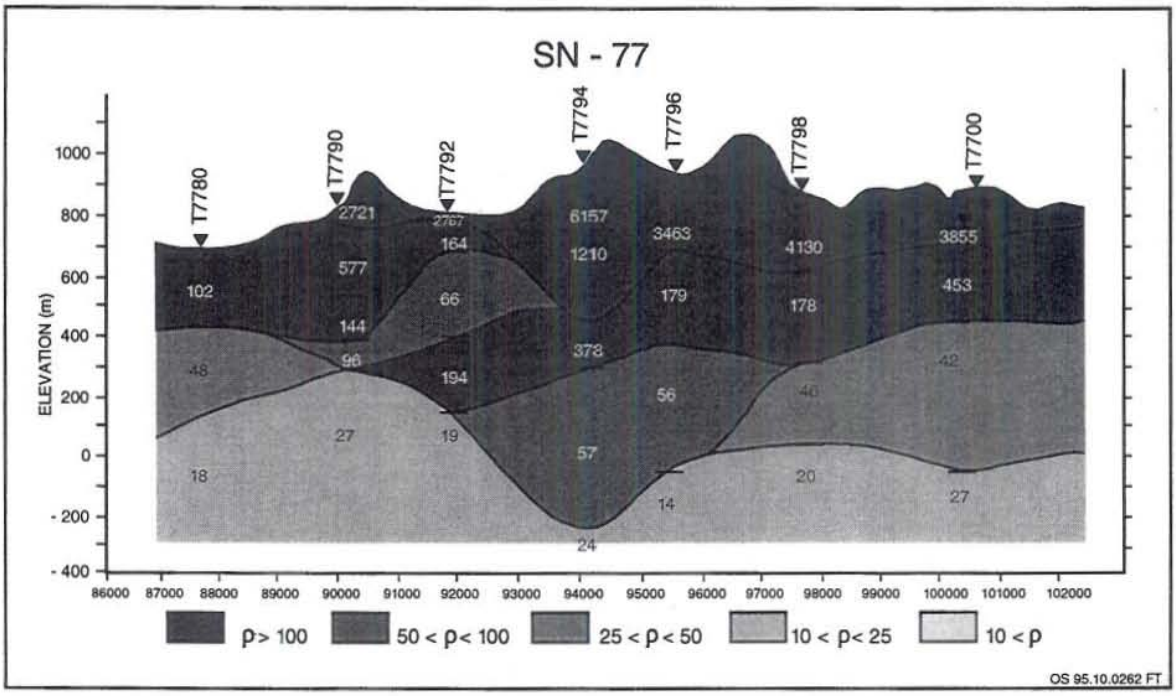

FIGURE 7: Resistivity cross-section SN-77

Resistivity cross-section SN83 (Figure 8)
The cross-section runs from south to north through the eastern part of the surveyed area with ten soundings projected on it. In the southern part, a high-resistivity layer of 100 to 512 Ωm overlies a thin conductive layer of resistivity lower than 10 Ωm. Below the thin layer lies a layer of relatively high resistivity (over 10 Ωm) and again higher resistivity at depth. In the northern part, a high-resistivity layer of over 100 Ωm is found at the surface. It overlies a low-resistivity layer of less than 10 Ωm. Higher resistivity is again observed at depth.

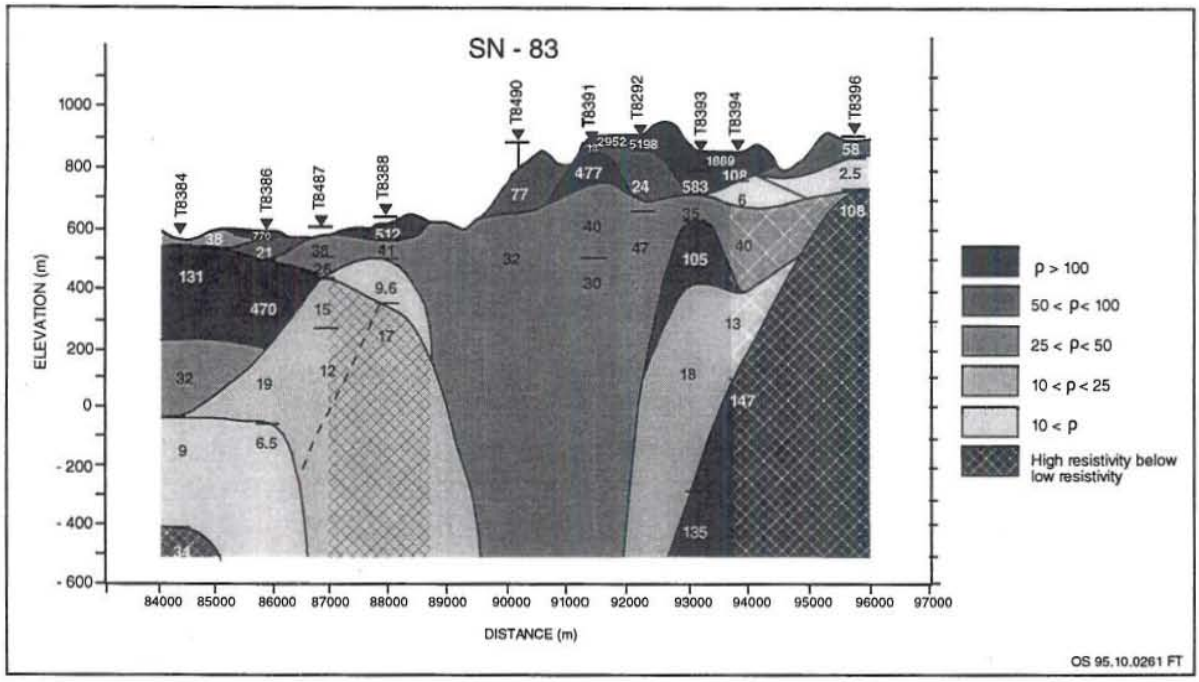

FIGURE 8: Resistivity cross-section SN-83

Resistivity cross-section WE 88 (Figure 9)

The cross-section runs from west to east in the southern path of the surveyed area with five soundings projected on it. A high-resistivity layer of 100 to 3000 Ωm was detected at the surface in all the soundings. Soundings T8187 and T8388, which are in the middle of the profile, show low-resistivity values. Soundings T7788, T8588 and T7988 which are on the extreme ends of the cross-section have resistivity values decreasing with depth. The low-resistivity layer that appears in the middle of the cross-section dips down to the west. The lowest resistivity values detected are 9.6 and 9.8 in soundings T7988 and T8388.

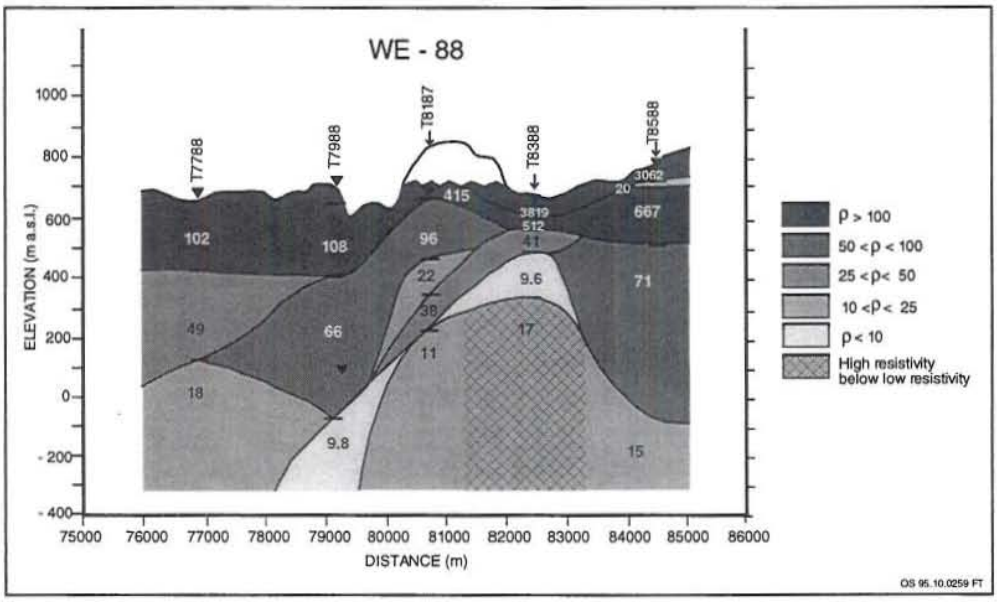

FIGURE 9: Resistivity cross-section WE-88

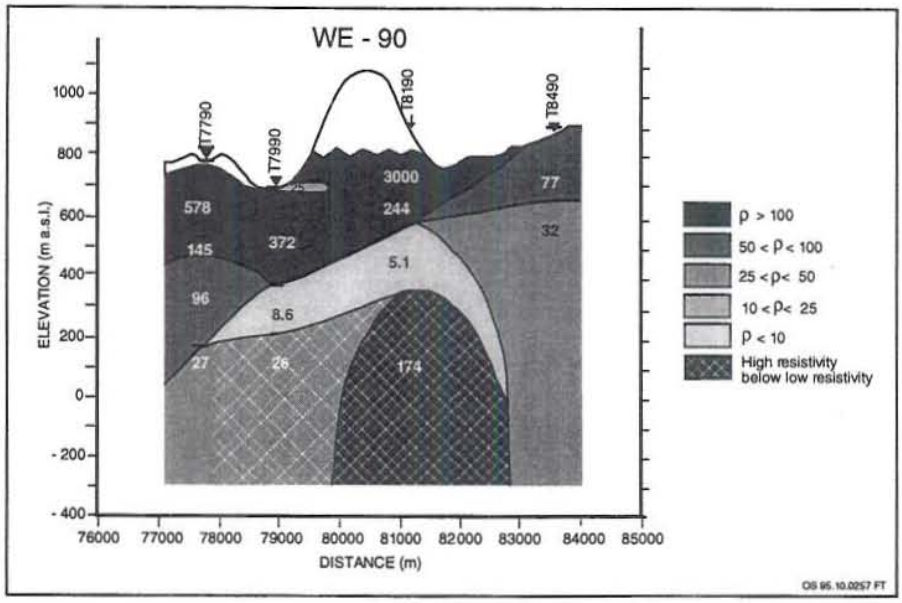

FIGURE 10: Resistivity cross-section WE-90

Resistivity cross-section WE 90 (Figure 10)
The cross-section runs from west to east with four soundings projected on it. A high-resistivity layer of over 100 to 3000 Ωm was detected with increasing thickness from east to west. A low-resistivity layer of resistivity less than 10 Ωm was detected in the middle of the profile in soundings T7990 and T8190. Below the low-resistivity layer a high-resistivity layer is observed. Extreme soundings on the cross-section have got resistivity values decreasing with depth.

Resistivity cross-section WE 92 (Figure 11)
The cross-section runs from west to east with six soundings projected on it. A high-resistivity layer of 100 to 3000 Ωm was found below the surface at both ends of the cross-section and connected by a thin layer near the surface in the middle. In soundings T7792, T8192 and T8292 a low-resistivity layer was detected dipping on both sides of sounding T8192 with a high-resistivity layer below it. Extreme soundings in the west of the cross-section have decreasing resistivity with depth. The lowest resistivity value detected is 2.1 Ωm in sounding T8192.

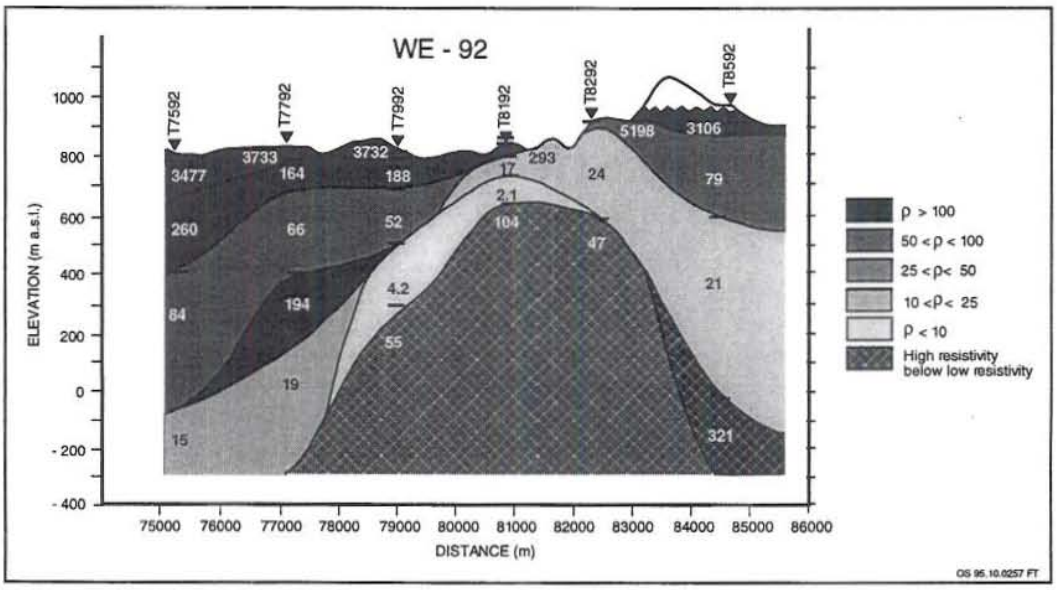

FIGURE 11: Resistivity cross-section WE-92

Resistivity cross-section WE 94 (Figure 12)
The cross-section runs from west to east with six soundings projected on it. A high-resistivity layer of 100 to 6000 Ωm was seen at the surface. A low-resistivity cap is clearly shown in the model. In the eastern part the low-resistivity layer appears near to the surface but dips gradually down between soundings T8394, T8294 and T8194 and steeply between soundings T7994 and T8194. In the western part, in sounding T7794, resistivity values decrease with depth. In other soundings the resistivity increases again below low-resistivity layer.

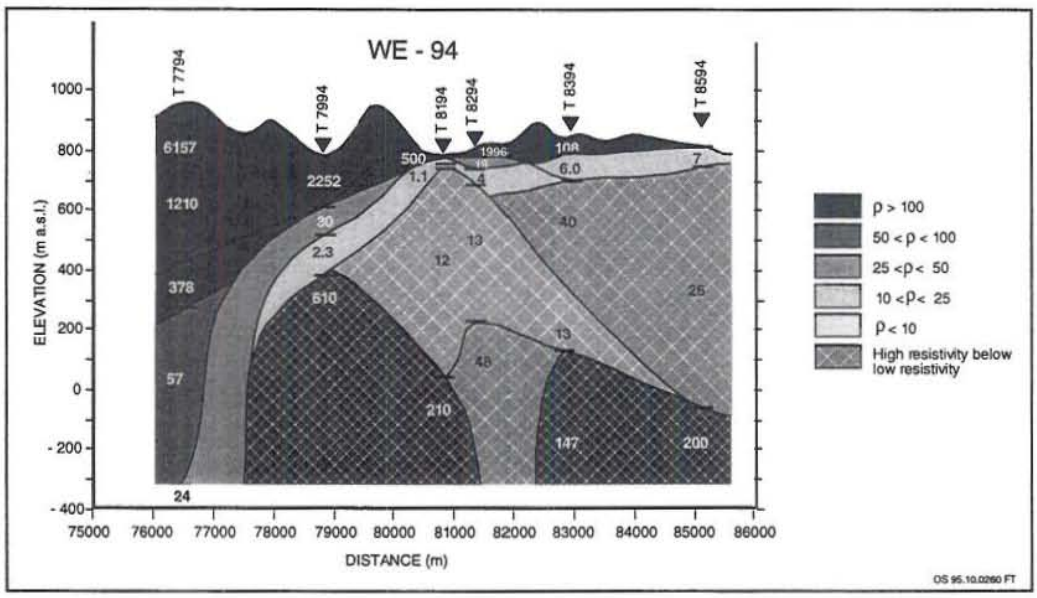

FIGURE 12: Resistivity cross-section WE-94

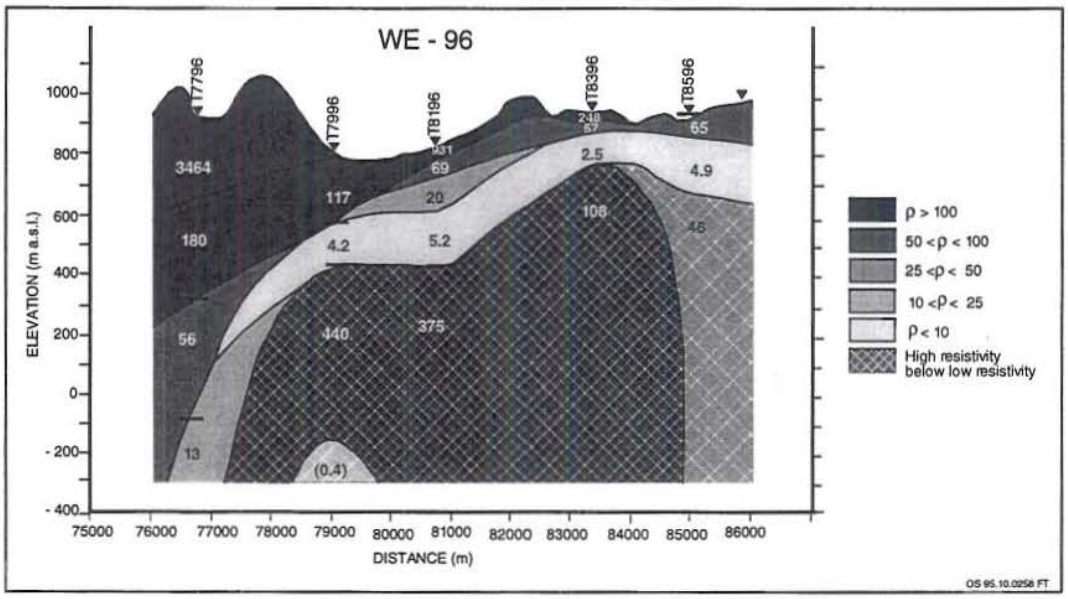

FIGURE 13: Resistivity cross-section WE-96

Resistivity cross-section WE 96 (Figure 13)
The cross-section runs from west to east with five soundings projected on it. In the western part in sounding T7796, resistivity values decrease with depth. A high-resistivity layer of 100 to 3000 Ωm was detected at the surface. The high-resistivity covers a low-resistivity layer with resistivity lower than 10 Ωm. Below this layer the resistivity increases again at depth.

7.3 Iso-resistivity maps

The iso-resistivity maps are based on the cross-sections described above. They were made at four different elevations, 700, 500, 300, and 100 m a.s.l. They show the general trend of resistivity at these elevations. Geothermal interpretation of these maps will be discussed in Chapter 7.4.

Iso-resistivity map at 700 m a.s.l. (Figure 14)
The map shows resistivity values higher than 100 Ωm in the western part of the surveyed area. Low-resistivity was observed in the middle part separating the high resistivity in the south and west and higher resistivity below low resistivity in the eastern part.

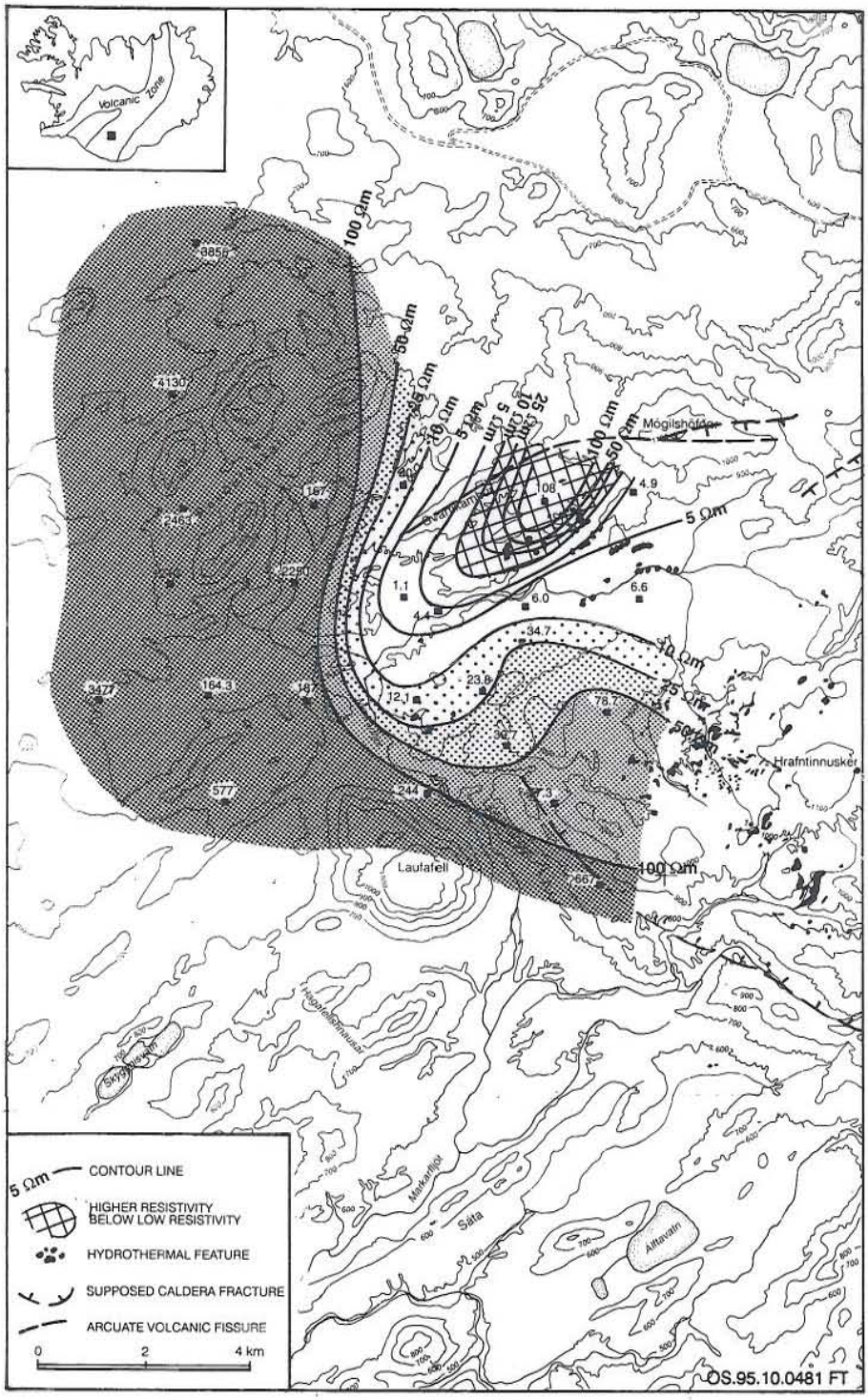

FIGURE 14: Iso-resistivity map of Torfajökull at 700 m above sea level

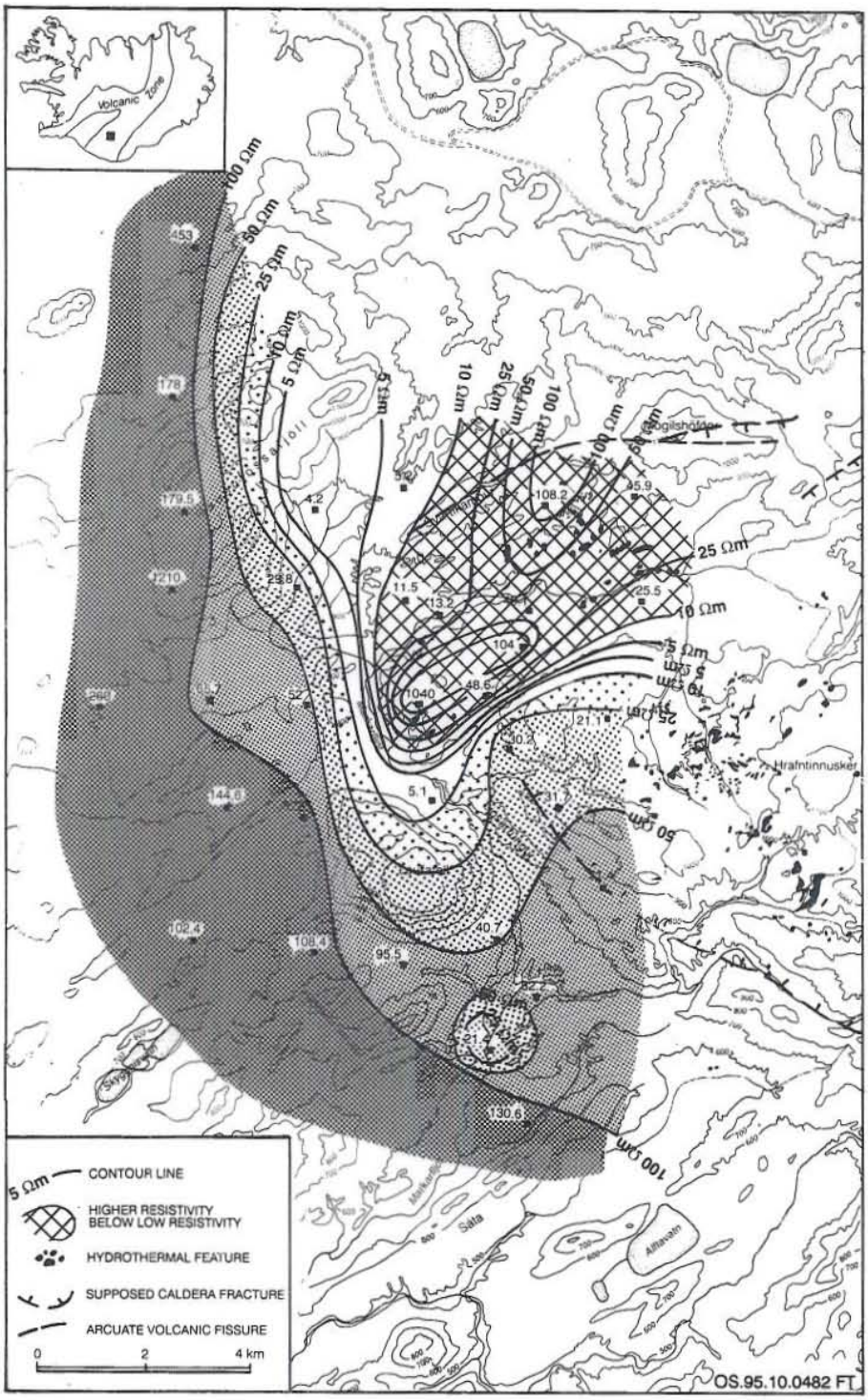

FIGURE 15: Iso-resistivity map of Torfajökull at 500 m above sea level

Iso-resistivity map at 500 m a.s.l. (Figure 15)

The map shows the same trend as that at 700 m a.s.l. except that the low-resistivity area has been shifted towards west and south. High resistivity is seen in the western part of the surveyed area. Low resistivity is seen in the middle. High resistivity below low resistivity is seen in the eastern part curving inside the low-resistivity area.

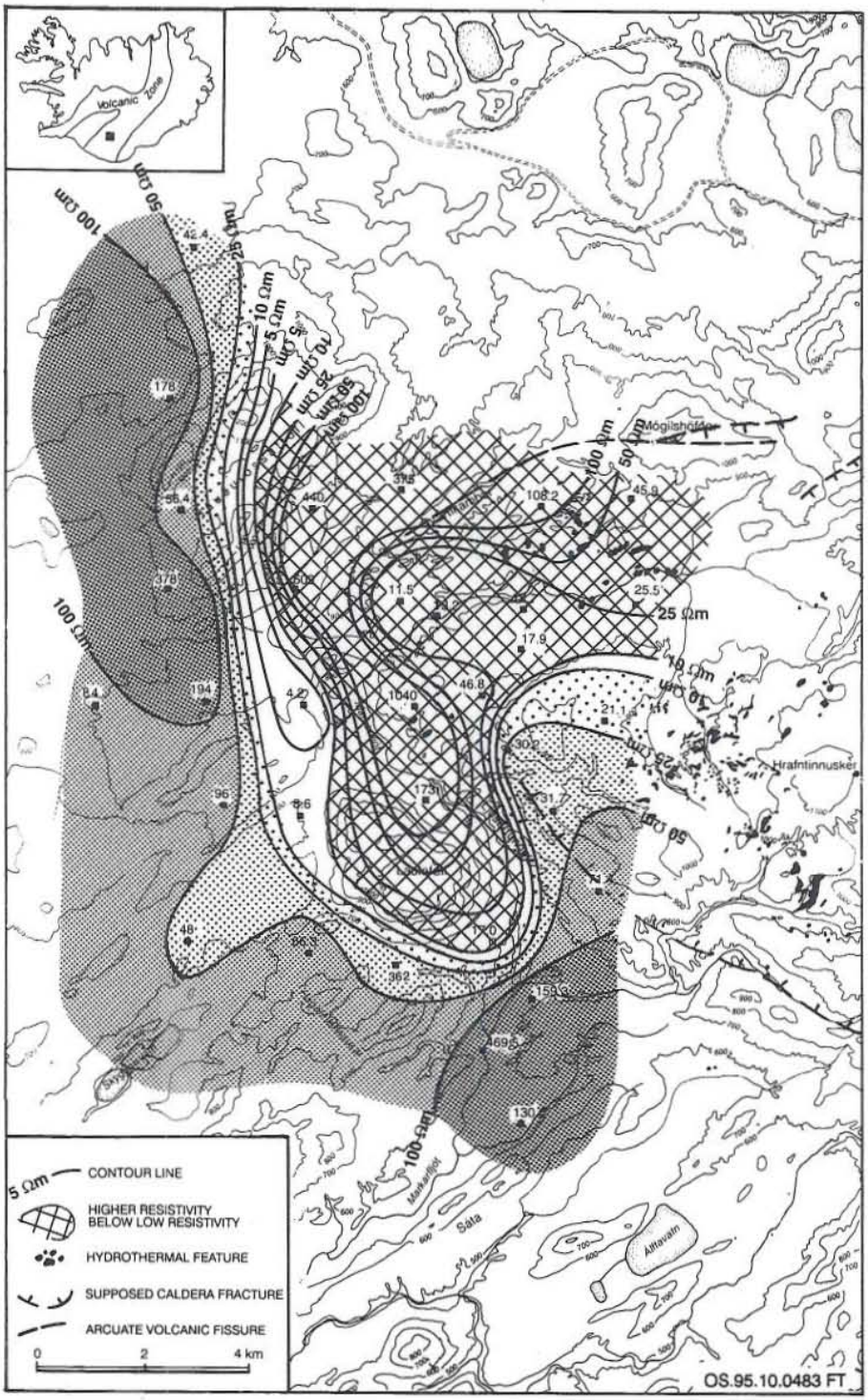

FIGURE 16: Iso-resistivity map of Torfajökull at 300 m above sea level

Iso-resistivity map at 300 m a.s.l. (Figure 16)
This map shows the same trend as the other maps at 700 and 500 m a.s.l. The low-resistivity area is extending further to the south and curves to the eastern side. The high resistivity below low resistivity has been extended further south. High resistivity is still found in the western part.

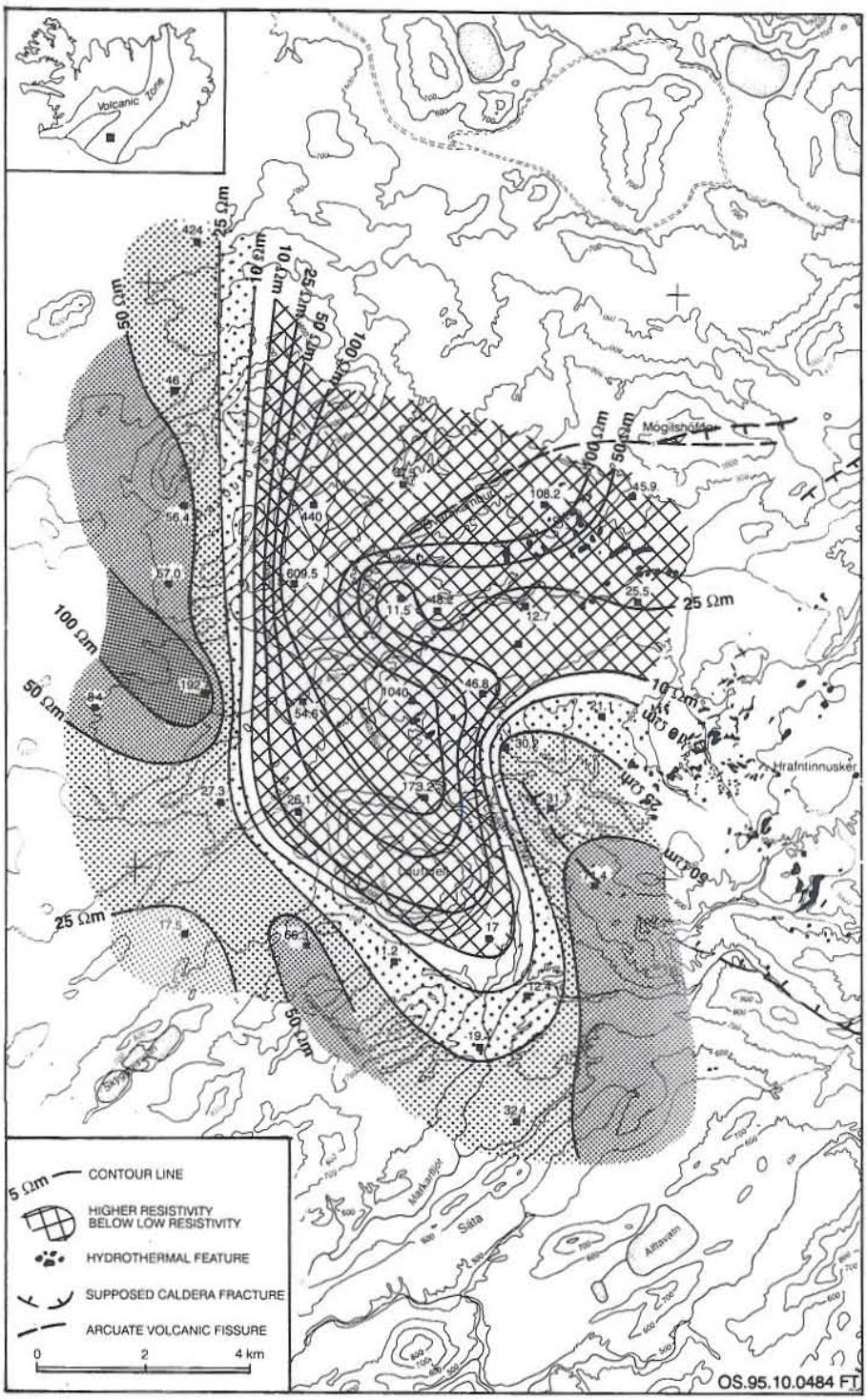

FIGURE 17: Iso-resistivity map of Torfajökull at 100 m above sea level

Iso-resistivity map at 100 m a.s.l. (Figure 17)
Like other maps this also shows a low-resistivity region in the middle separating the high resistivity in the west and the high resistivity below low resistivity in the east. The low-resistivity structure is extended further south. At this depth, the resistivity anomaly, consisting of low resistivity and higher resistivity below low resistivity, shows an arc-shaped structure in the central part of the area. This structure coincides roughly with the ring structure (caldera fault).

7.4 Geothermal interpretation

Comparison of alteration mineralogy and temperature in geothermal systems in Iceland has shown a consistent correlation (Árnason, 1993). If alteration is in equilibrium with temperature, cold rocks with temperature lower than 50°C are relatively fresh and unaltered. In the temperature range of 50-200°C alteration increases considerably and the dominant alteration minerals are smectite and zeolites. In the temperature range of 200-240°C zeolites mostly disappear and smectite gradually transforms into chlorite. This alteration zone is often called mixed layer clay zone. In the range of 240-250°C chlorite is found to be the dominant alteration mineral and above 250°C epidote and other high-temperature minerals are abundant. Resistivity surveys of fresh high-temperature geothermal systems in Iceland show a common resistivity structure. Below near surface resistive rocks, a low-resistivity cap of 1-10 Ωm is observed. Below the low-resistivity cap, the resistivity increases again, often by an order of magnitude or more. Comparison of this resistivity structure and alteration mineralogy shows that high-resistivity near surface reflects fresh rocks; the low-resistivity cap is found to coincide with the smectite-zeolite zone and the resistive core appears in the mixed layer clay and chlorite zone.

If alteration is in equilibrium with temperature, the resistivity can be interpreted in terms of likely temperatures. Resistive rocks, near surface, reflect cold rocks (T<50°C). The low-resistivity cap reflects temperatures in the range of 50-200°C on the outer margins of the geothermal systems and the resistive core corresponds to temperature about 240°C or higher, inside the geothermal systems.

The resistivity sections and iso-resistivity maps presented here show the same structure as described above and can therefore be interpreted in terms of geothermal activity in a relatively straightforward manner. The resistivity anomaly (low-resistivity cap and high-resistivity below low-resistivity) in the northeastern part of the surveyed area at 700 m a.s.l. shows that geothermal activity rises highest in this area. The anomaly correlates well with the abundant surface manifestations. It probably shows the top of an upward convecting geothermal plume with temperature of 240°C or higher. At greater depth the resistivity anomaly covers a considerably large area, reflecting larger extension of the geothermal system at depth. The iso-resistivity maps at 300 and 100 m a.s.l. show a clear arc-shaped resistivity anomaly with a well defined western boundary. This arc shaped anomaly roughly connects the caldera faults, as inferred from the geological investigations, through an area where geologists have not been able to map it. This strongly suggests that the anomaly associated with the geothermal activity is at the buried caldera fault.

The relationship between resistivity and temperature in high-temperature fields as described above cannot be applied blindly. For instance if the geothermal system has cooled down, it is likely that the old alteration dominates the resistivity distribution of the rocks, or if the system has been heated up recently it takes time for the mineralogy to respond to the increased temperature. It should also be kept in mind that the above discussed correlation between resistivity on the one hand, and alteration and temperature on the other is based on experience where basaltic rocks are dominant. It is possible that this correlation is not applicable in details where acidic rocks are abundant, like in the Torfajökull area. Therefore, the above described geothermal interpretation needs verification by exploratory drilling.

8. ADVANTAGES AND DISADVANTAGES OF THE TEM AND SCHLUMBERGER SOUNDING METHODS

When planning a geothermal resistivity survey, the choice of survey method is an important issue. This section briefly discusses the advantages and disadvantages of the resistivity methods discussed here.

The main advantages of the Schlumberger method are:

1. The method has been widely used for a long time and a lot of experience has been obtained;

2. The necessary equipment is relatively simple, cheap, and widely available;
3. The data collection process is "transparent" in the sense that measured signals can be visually inspected and a skilled operator can recognize anomalous function of equipment and take appropriate measures.

The main disadvantages of the Schlumberger method are:

1. In order to obtain a considerable depth of exploration, the current transmitting dipole has to be spread out to large distances. This makes the recorded signal dependent on a large volume of earth. The method is therefore sensitive to lateral variations in resistivity. Such lateral variations often make one-dimensional interpretation of sounding results in terms of layered models inadequate;
2. The sounding results can be badly affected by local resistivity anomalies around receiver dipole;
3. The large transmitter dipole, needed for deep soundings, can be a severe problem in areas of difficult topography and dense vegetation. Under such conditions, fieldwork is often greatly slowed down and much manpower may be needed;
4. In areas of dry and resistive surface, transmission of sufficient current to the ground, can be a difficult problem. This can makeSchlumberger soundings practically inapplicable in arid places;
5. Current leakage due to damaged insolation of the current transmission cables and spurious signals or drift from the potential electrodes of the receiver dipole can impose tricky problems. Such problems can be recognized by a skilled operator, but often they are not recognized, leading to severely contaminated or useless data.

The main advantages of the central-loop TEM soundings, as compared to Schlumberger soundings, are:

1. The data acquisition is cheaper and faster. In Iceland, TEM soundings are performed by a field crew of two or three men. For deep soundings (down to 600-1000 m) 300x300 m^2 square source loops are normally used. The time it takes to lay out the loop is minimal, compared to the time it takes to extend the current electrode spacing of the Schlumberger soundings to about 4000 m as is needed to get a similar depth of exploration. Laying out the source loop is a bit of hard labour since the wire is heavy, but once the loop is laid out, the data recording takes 30-60 minutes depending on signal to noise ratio. In Icelandic conditions a two-men field crew makes 2-3 TEM soundings per day, depending on the accessibility of sounding sites, but with Schlumberger soundings a field crew of four men makes 1-2 soundings a day.
2. No current has to be injected into the ground. This has proven to be very important where the surface is resistive, prohibiting good electrical contact with the ground.
3. Central-loop TEM soundings are much more downwards focused than Schlumberger soundings. This implies that one-dimensional inversion of TEM sounding is much better suited for resolving complicated resistivity structures than one-dimensional inversion of Schlumberger sounding.
4. The TEM method is relatively insensitive to local resistivity inhomogeneities at the sounding site, which can be a severe problem in Schlumberger soundings.

The main disadvantages of the TEM method are:

1. The sounding equipment is electronically sophisticated and relatively expensive. Repairing and maintenance often requires very skilled electronic engineers. However, much of the TEM equipment, on the market has been found to be reliable and not needing much maintenance.
2. The data acquisition is highly automatized and not very "transparent". This means that malfunction in the instruments or corrupted data is not as easily recognized as in the more transparent data collection in the Schlumberger soundings. The automatization of the data collection can, on the other hand, prevent human errors.
3. The equipment is rather bulky, comprising a transmitter, a receiver, a motor generator and the wire for the source loop. The total weight of the equipment is generally about 200 kg.
4. Because the TEM method is based on the recording of transient magnetic fields, the method is very sensitive to broad band electromagnetic noise. The method is therefore hard to apply close to power lines and other places with much electromagnetic noise.

9. CONCLUSIONS

General aspects of the geothermal exploration have been discussed briefly. Resistivity methods are found to be among the most important surface exploration methods. The usefulness relies on the fact that resistivity is the most diagnostic parameter related to the geothermal resources that can be measured by surface exploration

Two resistivity methods have been discussed in some details, i.e. Schlumberger and TEM soundings. These methods have been developed to such a stage that they are used routinely in geothermal exploration and Schlumberger soundings have been used for a long time. In routine use, the sounding results are normally interpreted in terms of layered-earth models by one-dimensional inversion. The basic ingredients of the inversion programmes for these methods, the solution to the forward problem and inversion algorithms, have been discussed.

Resistivity data, both using the Schlumberger and TEM method , from the Torfajökull geothermal field in South Iceland have been interpreted by one-dimensional inversion. The Schlumberger data, which are more than 20 years old, were found to be of low quality and did not add any information to the more recent TEM data. The one-dimensional models of the 33 TEM soundings have been used to compile resistivity cross-sections through the surveyed area and iso-resistivity maps at different depths. The cross-sections and maps show a clear low-resistivity cap overlying a more resistive core, having the same general structure as found in many other high-temperature geothermal systems in Iceland. The resistive structure is interpreted, based on experience in other geothermal fields, in terms geothermal parameters, such as likely upflow zones and temperature. This interpretation indicates temperatures higher than 240°C in the reservoir and the distribution is believed to indicate connection to a buried caldera fault under the surveyed area.

ACKNOWLEDGEMENTS

Thanks are due to the administration of the UNU Geothermal Training Programme. The director Dr. Ingvar Fridleifsson for organizing the programme. To his deputy, Lúdvík S. Georgsson who confirmed my coming to attend this programme, Súsanna Westlund and Margrét Westlund for there willingness to help the Fellows. To the Orkustofnun staff for the lectures during the introductory part of the course. Special thanks are due to the geophysical section for the lectures during the specialised training and field work. Grateful thanks are due to my supervisor Knútur Árnason for his unselfish, untiring efforts and critical comments during all the time that went into the preparation of this report. Thanks to Helga, Audur and Sylvía in the drawing room who worked tirelessly on the drawings.

Thanks to the administration of Geological Survey and Mines Department of Uganda especially the geothermal group for accepting my application. I thank greatly my family and all the people who sustained my absence and prayed for me during the six months of the training.

REFERENCES

Archie, G.E., 1942: The electrical resistivity log as an aid in determining some reservoir characteristics. *Tran. AIME, 146,* 54-67.

Arnórsson, S., Ívarsson, G., Cuff, K.V., and Saemundsson, K., 1987: Geothermal activity in the Torfajökull field, South Iceland: Summary of geochemical studies. *Jökull, 37,* 1-11.

Árnason, K., 1984: The effect of finite electrode separation on Schlumberger soundings. *54th Annual International SEG Meeting, Atlanta, Expanded Abstracts,* 129-132.

Árnason, K., 1989: *Central loop transient electromagnetic sounding over a horizontally layered earth.* Orkustofnun, Reykjavík, report OS-89032/JHD-06, 128 pp.

Árnason, K., 1993: Relation between resistivity and geothermal activity in basaltic rocks. English translation of a chapter in: *Geothermal activity at the Ölkelduháls field, resistivity soundings in 1991 and 1992.* Orkustofnun, Reykjavík, report OS-93037/JHD-10 (in Icelandic), 82 pp.

Árnason, K., and Flóvenz, Ó.G., 1992: Evaluation of physical methods in geothermal exploration of rifted volcanic crust. *Geoth. Res. Council, Transactions, 16,* 207-214.

Árnason, K., and Hersir, G.P., 1988: *One-dimensional inversion of Schlumberger resistivity soundings. Computer program, description and user's guide.* UNU G.T.P., Iceland, report 8, 59 pp.

Dakhnov, V.N., 1962: Geophysical well logging. *Q. Colorado Sch. Mines, 57-2,* 445 pp.

Eysteinsson, H., Árnason, K., Flóvenz, Ó.G., 1993: Resistivity methods in geothermal prospecting in Iceland. *Surveys in Geophysics, 15,* 263-275.

Flóvenz, Ó.G., Georgsson, L.S., and Árnason, K., 1985: Resistivity structure of the upper crust in Iceland. *J. Geophys. Res., 90-B12,* 10136-10150.

Georgsson, L.S., 1984: Resistivity and temperature distribution of the outer Reykjanes Peninsula, Southwest Iceland. *54th Annual International SEG Meeting, Atlanta, Expanded Abstracts,* 81-84.

Hersir, G.P., and Björnsson, A., 1991: *Geophysical exploration for geothermal resources, principles and applications.* UNU G.T.P., Iceland, report 15, 94 pp.

Ívarsson, G., 1992: *Geology and petrochemistry of the Torfajökull central volcano in Central South Iceland, in association with the Icelandic hot spot and rift zones.* Ph.D. thesis, University of Hawaii, Hawaii, 319 pp.

Kaufman, A.A., and Keller, G.V., 1981: *The magnetotelluric sounding method.* Elsevier Scientific Publishing Co., Amsterdam, 595 pp.

Keller, G.V., and Frischknecht, F.C., 1966: *Electrical methods in geophysical prospecting.* Pergamon Press, Oxford, 527 pp.

Koefoed, O., 1979: *Geosounding principles, 1: Resistivity sounding measurements.* Elsevier Scientific Publishing Co., Amsterdam, 276 pp.

Kristmannsdóttir, H., 1979: Alteration of basaltic rocks by hydrothermal activity at 100-300°C. In: Mortland, M.M., and Farmer, V.C. (editors), *International Clay Conference 1978.* Elsevier Scientific Publishing Co., Amsterdam, 359-367.

Pálmason, 1980: Geothermal activity as an energy source (in Icelandic). *Náttúrufraedingurinn, 50-3/4,*147-156.

Stefánsson, V., Axelsson, G., and Sigurdsson, Ó., 1982: Resistivity logging of fractured basalt. *Proceedings of the 8th Workshop on Geothermal Reservoir Engineering, Stanford University, California,* 189-195.

APPENDIX I: TEM soundings from Torfajökull with 1-dimensional interpretation

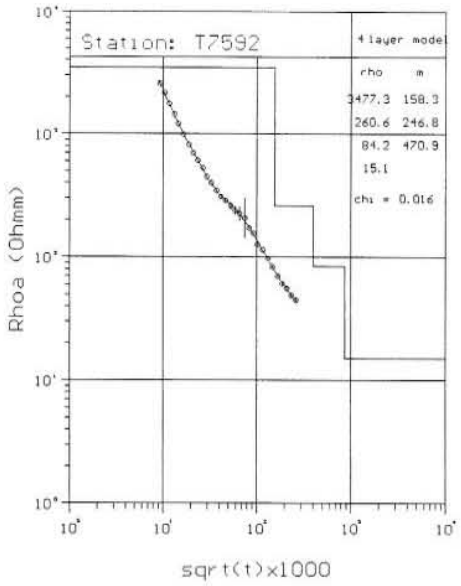

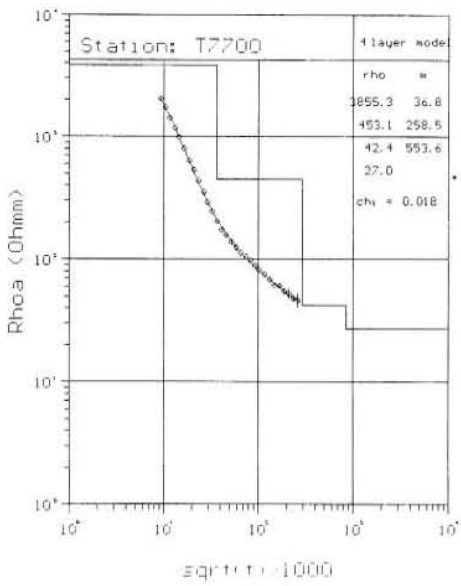

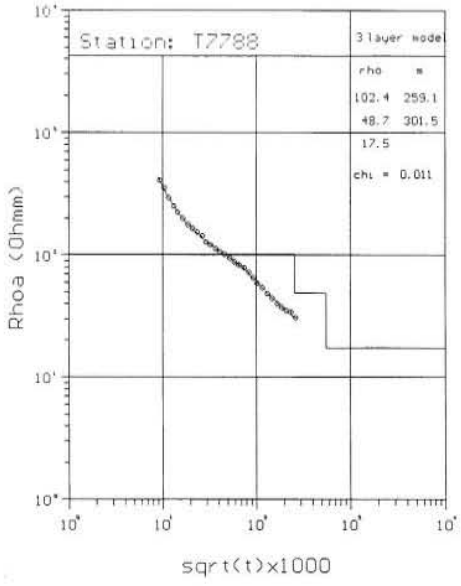

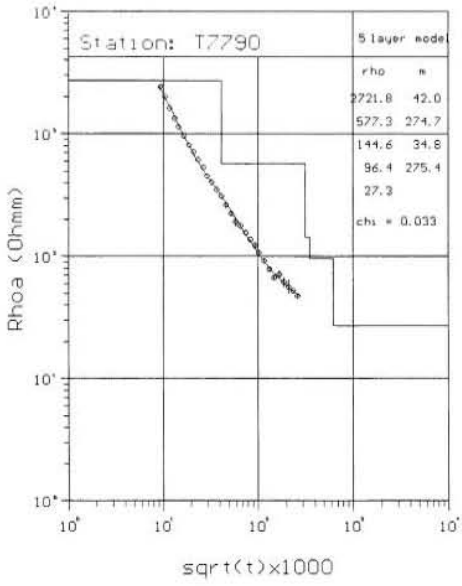

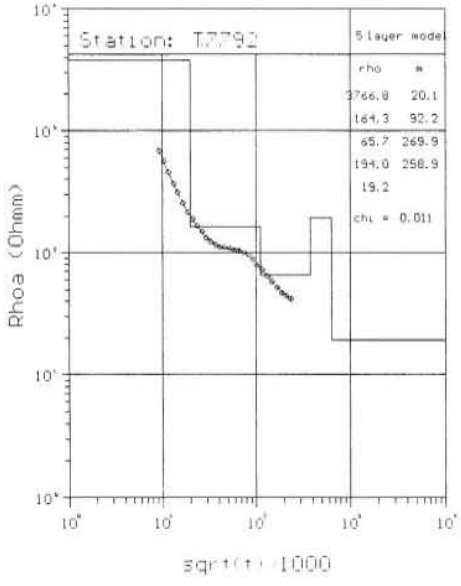

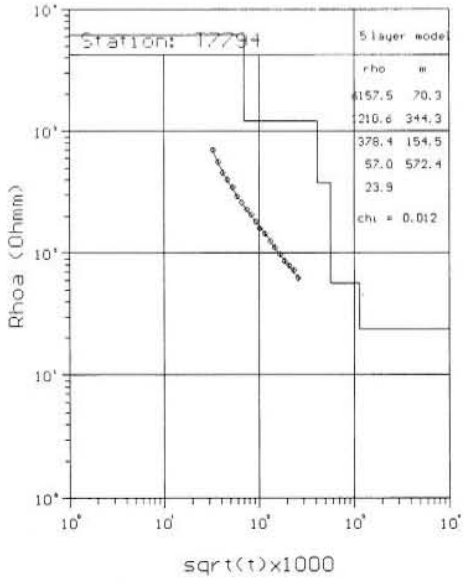

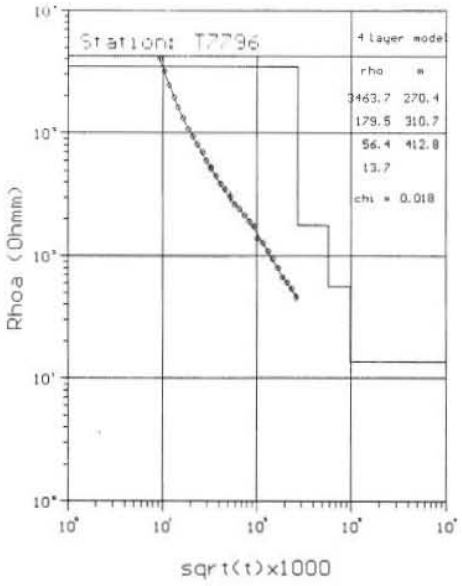
Station: T7796
4 layer model
rho m
3463.7 270.4
179.5 310.7
56.4 412.8
13.7
chi = 0.018
Rhoa (Ohmm)
sqrt(t)x1000

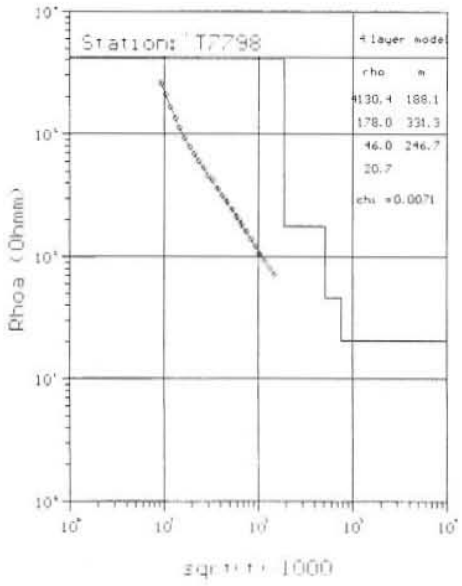
Station: T7798
4 layer model
rho m
4130.4 188.1
178.0 331.3
46.0 246.7
20.7
chi =0.0071
Rhoa (Ohmm)
sqrt(t)x1000

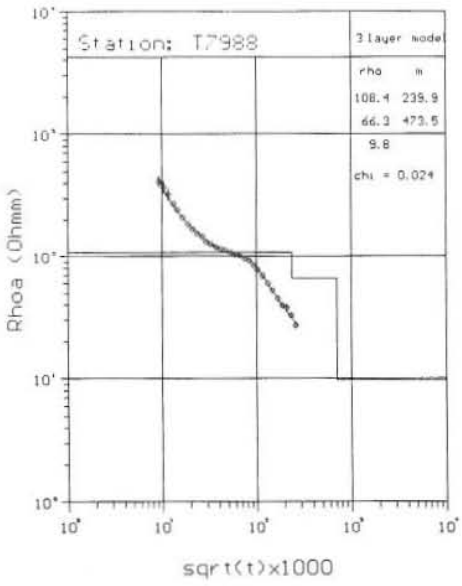
Station: T7988
3 layer model
rho m
108.4 239.9
66.3 473.5
9.8
chi = 0.024
Rhoa (Ohmm)
sqrt(t)x1000

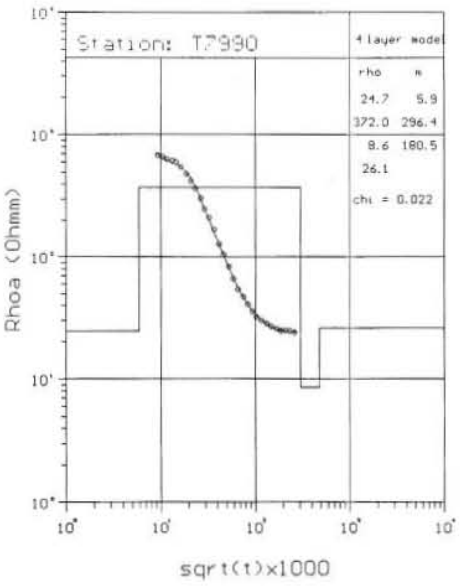
Station: T7990
4 layer model
rho m
24.7 5.9
372.0 296.4
8.6 180.5
26.1
chi = 0.022
Rhoa (Ohmm)
sqrt(t)x1000

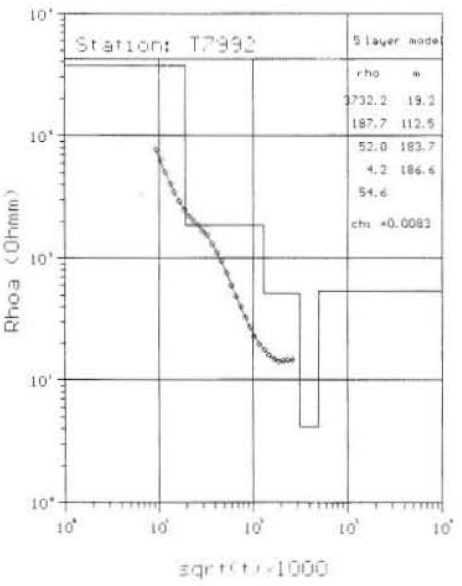
Station: T7992
5 layer model
rho m
1732.2 19.2
187.7 112.5
52.0 183.7
4.2 186.6
54.6
chi =0.0083
Rhoa (Ohmm)
sqrt(t)x1000

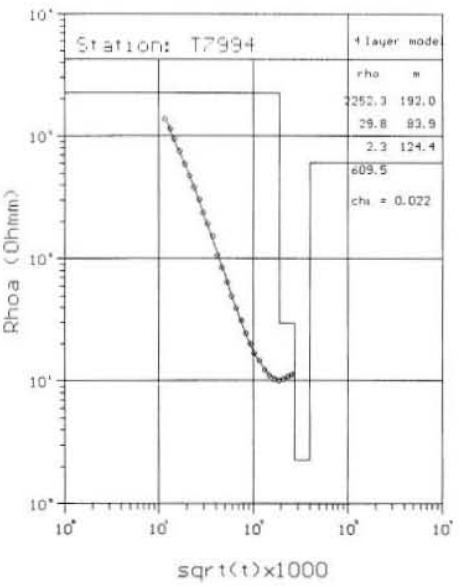
Station: T7994
4 layer model
rho m
2252.3 192.0
29.8 83.9
2.3 124.4
609.5
chi = 0.022
Rhoa (Ohmm)
sqrt(t)x1000

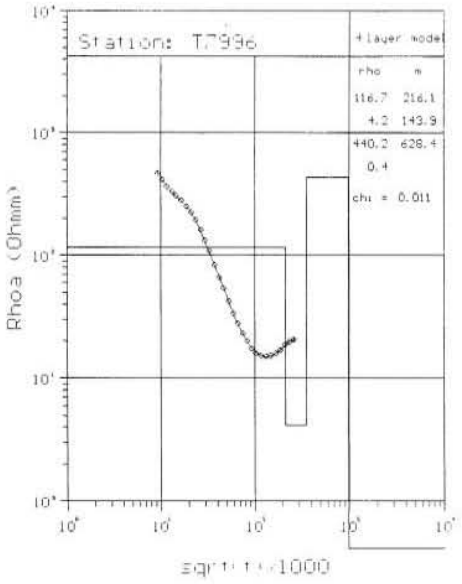
Station: T7996
4 layer model
rho m
116.7 216.1
4.2 143.9
440.2 628.4
0.4
chi = 0.011
Rhoa (Ohmm)
sqrt(t)x1000

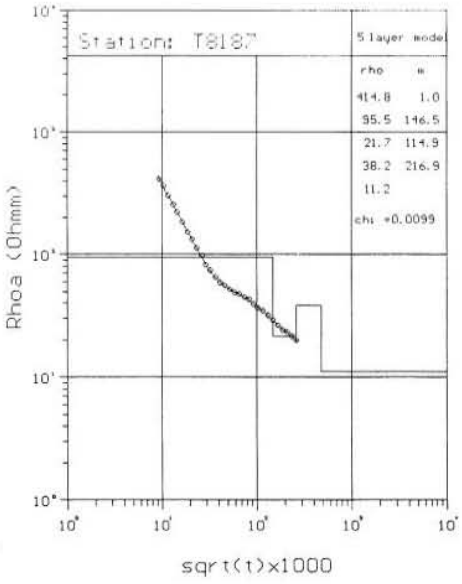
Station: T8187
5 layer model
rho m
414.8 1.0
95.5 146.5
21.7 114.9
38.2 216.9
11.2
chi =0.0099
Rhoa (Ohmm)
sqrt(t)x1000

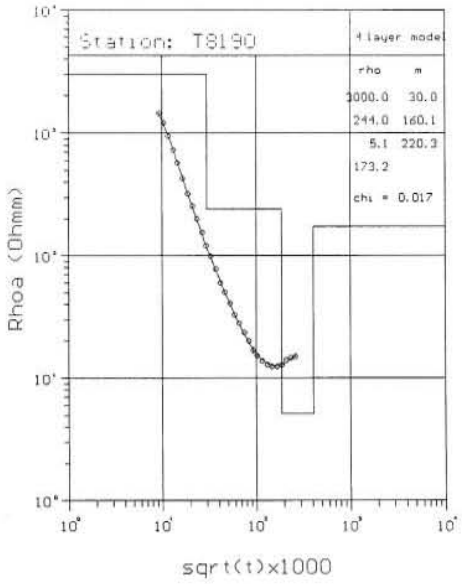
Station: T8190
4 layer model
rho m
3000.0 30.0
244.0 160.1
5.1 220.3
173.2
chi = 0.017
Rhoa (Ohmm)
sqrt(t)x1000

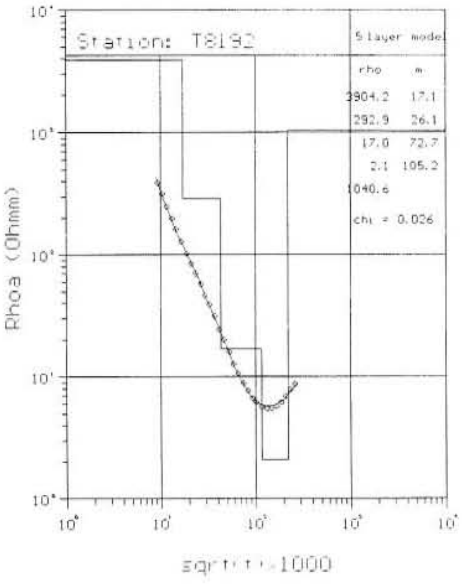
Station: T8192
5 layer model
rho m
3904.2 17.1
292.9 26.1
17.0 72.7
2.1 105.2
1040.6
chi = 0.026
Rhoa (Ohmm)
sqrt(t)x1000

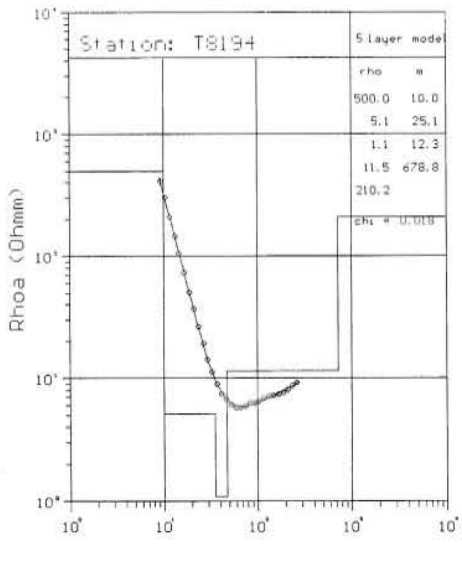
Station: T8194
5 layer model
rho m
500.0 10.0
5.1 25.1
1.1 12.3
11.5 678.8
210.2
chi = 0.018
Rhoa (Ohmm)

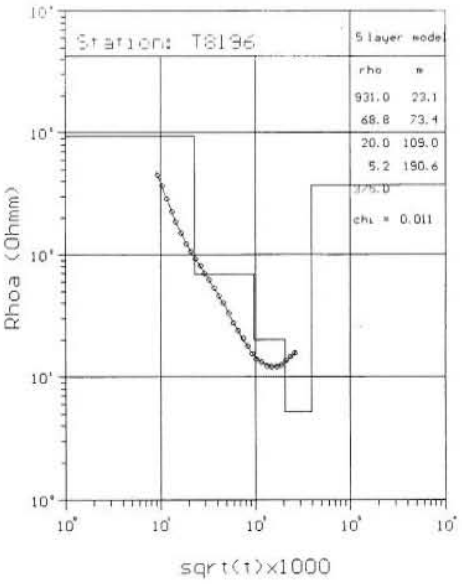
Station: T8196
5 layer model
rho m
931.0 23.1
68.8 73.4
20.0 109.0
5.2 190.6
375.0
chi = 0.011
Rhoa (Ohmm)
sqrt(t)x1000

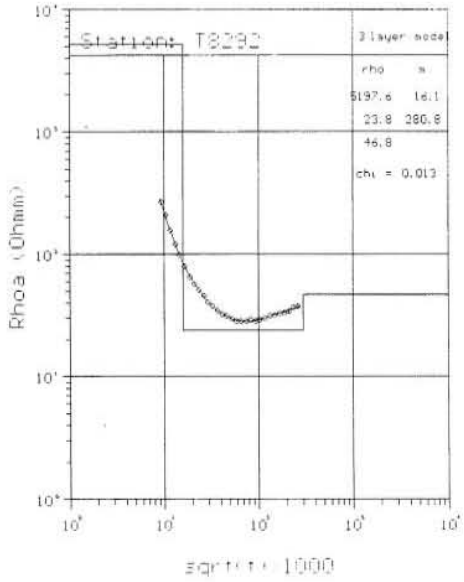
Station: T8293
3 layer model
rho m
5197.6 16.1
23.8 280.8
46.8
chi = 0.013
Rhoa (Ohmm)
sqrt(t)x1000

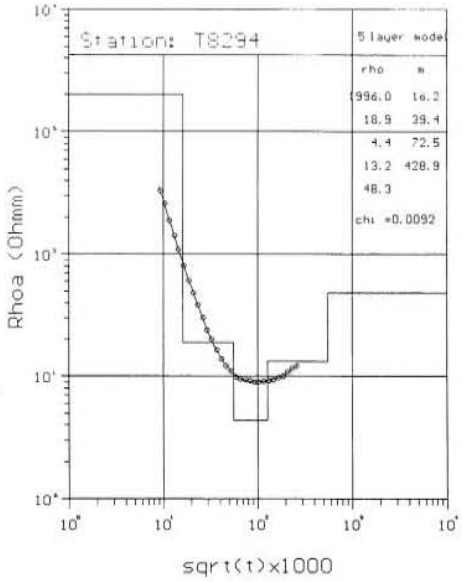
Station: T8294
5 layer model
rho m
996.0 16.2
18.9 39.4
4.4 72.5
13.2 428.9
48.3
chi =0.0092
Rhoa (Ohmm)
sqrt(t)x1000

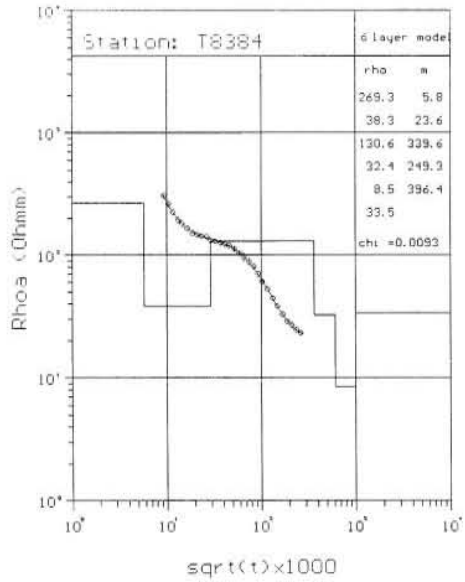
Station: T8384
6 layer model
rho m
269.3 5.8
38.3 23.6
130.6 339.6
32.4 249.3
8.5 396.4
33.5
chi =0.0093
Rhoa (Ohmm)
sqrt(t)x1000

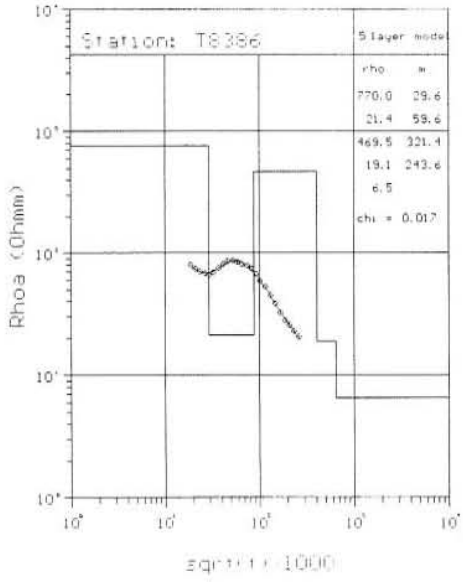
Station: T8386
5 layer model
rho m
770.0 29.6
21.4 59.6
469.5 321.4
19.1 243.6
6.5
chi = 0.017
Rhoa (Ohmm)
sqrt(t)x1000

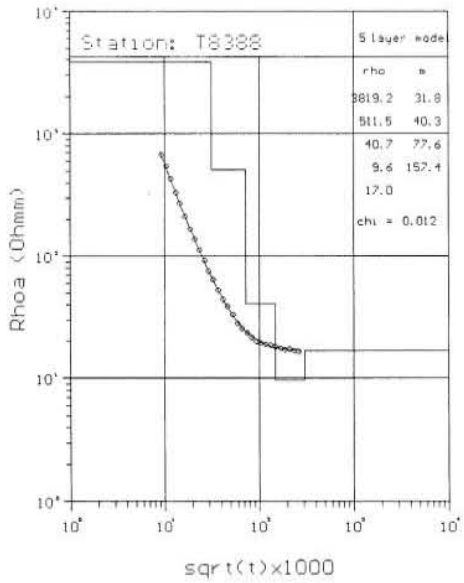
Station: T8388
5 layer model
rho m
3819.2 31.8
511.5 40.3
40.7 77.6
9.6 152.4
17.0
chi = 0.012
Rhoa (Ohmm)
sqrt(t)x1000

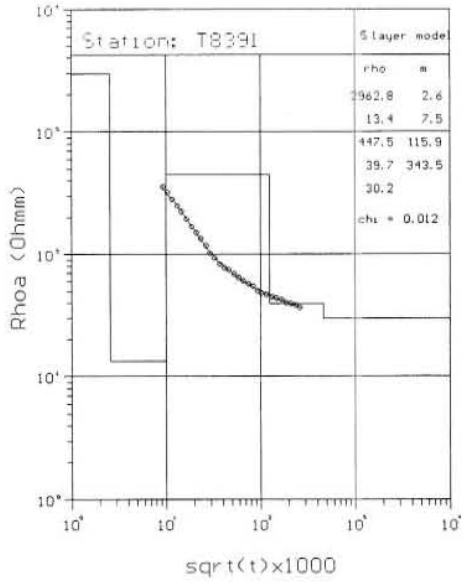
Station: T8391
5 layer model
rho m
2962.8 2.6
13.4 7.5
447.5 115.9
39.7 343.5
30.2
chi = 0.012
Rhoa (Ohmm)
sqrt(t)x1000

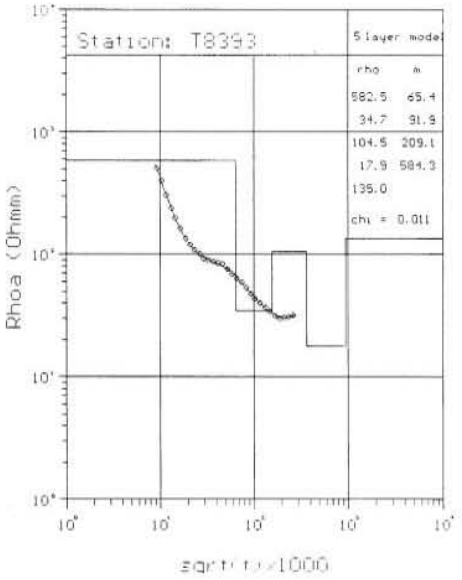
Station: T8393
5 layer model
rho h
582.5 65.4
34.7 91.9
104.5 209.1
17.9 584.3
135.0
chi = 0.011
Rhoa (Ohmm)
sqrt(t)x1000

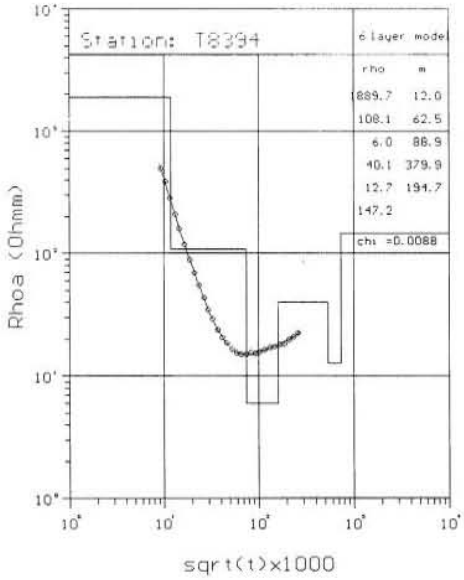
Station: T8394
6 layer model
rho h
889.7 12.0
108.1 62.5
6.0 88.9
40.1 379.9
12.7 194.7
147.2
chi =0.0088
Rhoa (Ohmm)
sqrt(t)x1000

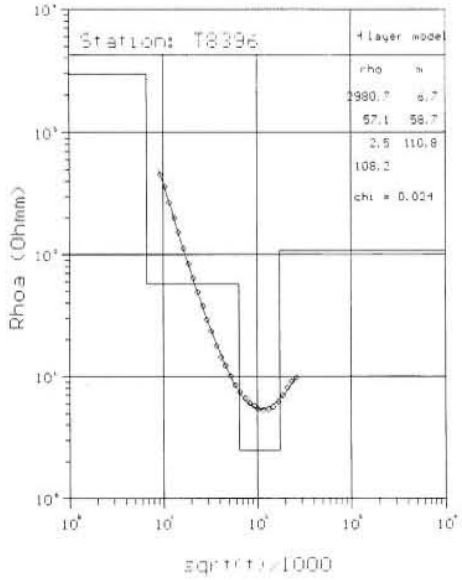
Station: T8396
4 layer model
rho h
2980.7 6.7
57.1 58.7
2.5 110.8
108.2
chi = 0.024
Rhoa (Ohmm)
sqrt(t)x1000

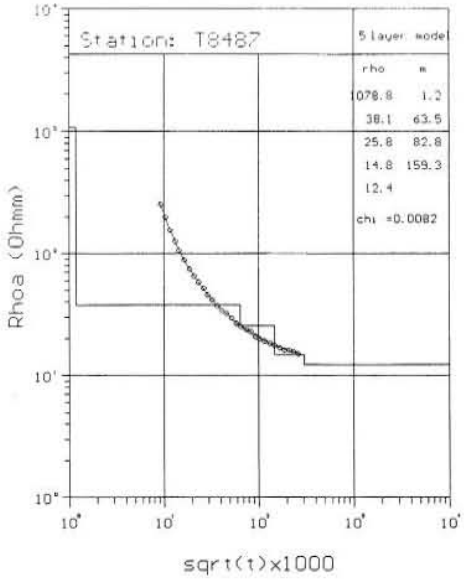
Station: T8487
5 layer model
rho h
1078.8 1.2
38.1 63.5
25.8 82.8
14.8 159.3
12.4
chi =0.0082
Rhoa (Ohmm)
sqrt(t)x1000

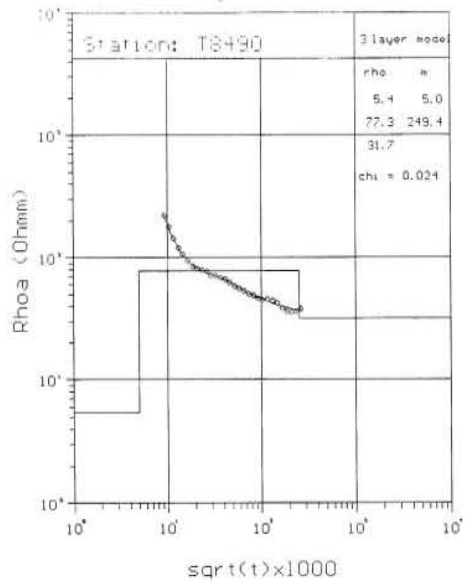
Station: T8490
3 layer model
rho h
5.4 5.0
77.3 249.4
31.7
chi = 0.024
Rhoa (Ohmm)
sqrt(t)x1000

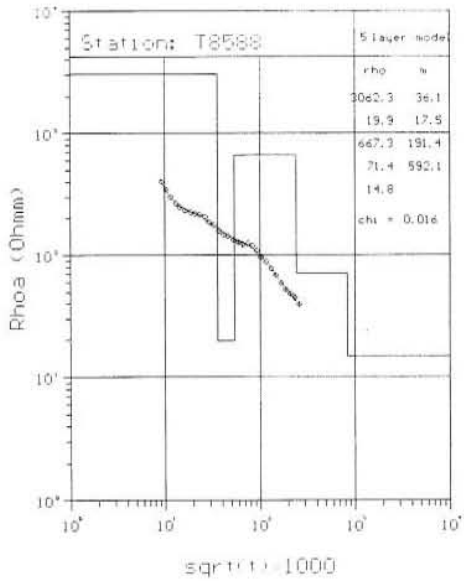
Station: T8588
5 layer model
rho h
3062.3 36.1
19.9 17.5
667.3 191.4
71.4 592.1
14.8
chi = 0.016
Rhoa (Ohmm)
sqrt(t)x1000

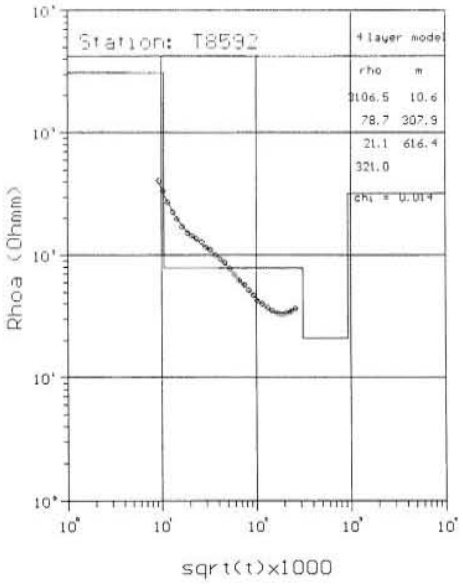
Station: T8592
4 layer model
rho m
2106.5 10.6
78.7 307.9
21.1 616.4
321.0
chi = 0.014
Rhoa (Ohmm)
sqrt(t)x1000

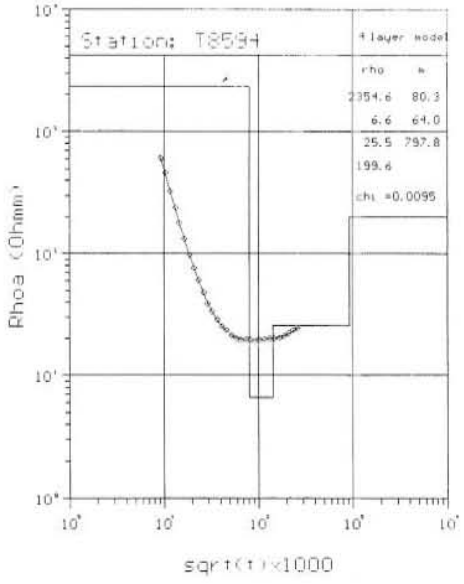
Station: T8594
4 layer model
rho m
2354.6 80.3
6.6 64.0
25.5 797.8
199.6
chi =0.0095
Rhoa (Ohmm)
sqrt(t)x1000

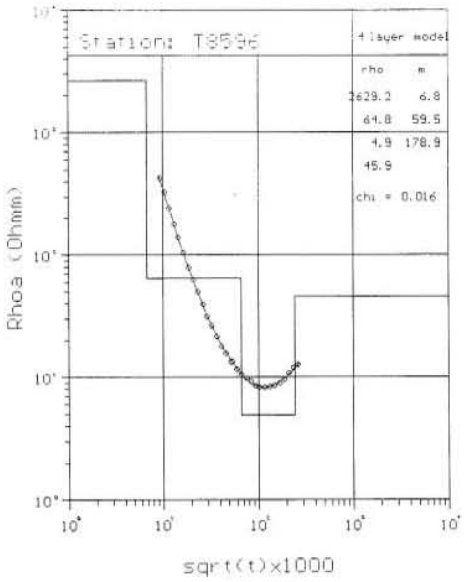
Station: T8596
4 layer model
rho m
2629.2 6.8
64.8 59.5
4.9 178.9
45.9
chi = 0.016
Rhoa (Ohmm)
sqrt(t)x1000